SECTION PAGE

SECTION **PAGE**

LIST OF TABLES

LIST OF FIGURES

CHAPTER 4

THERMAL EVALUATION

4.1 Discussion

The TN-68 cask is designed to passively reject decay heat under normal storage, accident, and loading/unloading conditions while maintaining temperatures and pressures within specified limits. Objectives of the thermal analyses performed for this evaluation include:

- Determination of maximum and minimum temperatures with respect to cask material limits to ensure components perform their intended safety functions;
- Determination of temperature distributions to support the calculation of thermal stresses;
- Determination of maximum cask internal pressures for normal, off-normal, and accident conditions, and
- Determination of the maximum fuel cladding temperature, and to confirm that this temperature will remain sufficiently low to prevent unacceptable degradation of the fuel during storage.

To establish the heat removal capability, several thermal design criteria are established for the system. These are:

- Maximum temperatures of the containment structural components must not adversely affect the containment function.
- A maximum fuel cladding temperature limit of 400^{o}C (752^{o}F) is considered for normal conditions of storage and for short-term storage operations such as vacuum drying. During off-normal storage and accident conditions, the fuel cladding temperature limit is 570^{o}C (1058^{o}F). These limits are based on the NRC recommendations in ISG-11, rev. 3 [1].
- A maximum temperature limit of 536^{o}F (280^{o}C) is set for the Helicoflex seals (double metallic seals) in the containment vessel closure lid to satisfy the leak tight containment function.
- A maximum allowable temperature of 300^{o}F is considered for the radial neutron shield. The maximum allowable limit for the top neutron shield is 220^{o}F for long term and 300^{o}F for short term conditions.
- The minimum and maximum ambient temperatures during handling and storage are -20^{o}F (-29°C) and 115^{o}F (46°C) respectively. In general, all the thermal criteria are associated with maximum temperature limits and not minimum temperatures. All

materials can be subjected to a minimum environment temperature of -20°F (-29°C) without adverse effects.

- The maximum cask internal pressure for all conditions must be below the design pressure of 100 psig.

The TN-68 cask is analyzed based on a maximum heat load of 30 kW from 68 fuel assemblies with a maximum decay heat of 0.441 kW per fuel assembly.

A description of the detailed analyses performed for normal/off-normal conditions is provided in Section 4.3, and accident conditions in Section 4.4. The thermal analyses performed for the loading and unloading conditions are described in Section 4.5. The effects of the damaged fuel assemblies on thermal performance are discussed in Section 4.6. The cask internal pressures are discussed in Section 4.7.

Fuel assemblies are considered as homogenized materials in the fuel compartments. The effective thermal conductivity of the fuel assemblies used in the thermal analysis is based on the conservative assumption that heat transfer within the fuel region occurs only by conduction and radiation where any convection heat transfer is neglected. The lowest effective properties among the applicable fuel assemblies are selected to perform the thermal analysis. Section 4.8 presents the calculation that determines the bounding effective thermal properties of the applicable fuel assemblies.

The analyses consider the effect of the decay heat flux varying axially along the active fuel length. The axial decay heat profile for a BWR fuel assembly is based on measured data from Reference [4]. Section 4.9 describes the calculated peaking factors and the methodology to apply the axial heat profile in the model.

The thermal evaluation concludes that with a design basis heat load of 30 kW all design criteria are satisfied.

4.2 Summary of Thermal Properties of Materials

The analyses use interpolated values when appropriate for intermediate temperatures where the temperature dependency of a specific parameter is deemed significant. The interpolation assumes a linear relationship between the reported values. The material properties of metallic alloys are based on ASME code 1998 and 200 addenda [5].

1. Homogenized Intact BWR Fuel [1]

Temp	Transverse conductivity in Helium	Temp	Transverse Conductivity for Vacuum Conditions
(°F)	(Btu/hr-in -°F)	(°F)	(Btu/hr-in-°F)
128	0.01340	178	0.0049
224	0.0162	263	0.0062
321	0.0188	350	0.0077
418	0.0217	440	0.0096
515	0.0251	533	0.0118
613	0.0290	627	0.0145
712	0.0331	722	0.0176
810	0.0377	818	0.0211
909	0.0427	915	0.0252
1008	0.0483	1013	0.0297
1107	0.0552	1111	0.0351

k_{eff} – axial = 0.0449 Btu/hr-in-°F
ρ_{eff} = 0.105 lbm/in^3
Cp_{eff} = 0.0576 Btu/lbm-°F

2. Homogenized Damaged BWR Fuel [1]

Temp	Transverse conductivity in Helium
(°F)	(Btu/hr-in -°F)
120	0.0113
217	0.0133
315	0.0156
413	0.0182
511	0.0212
609	0.0246

keff – axial = 0.0449 x 0.9 = 0.0404 Btu/hr-in-°F

[1] See Section 4.8 for calculation of the effective properties

3. Helium [4]

Temperature		Conductivity	
(K)	(°F)	(W/m-K)	(Btu/hr-in-°F)
200	-100	0.1151	0.0055
250	-10	0.1338	0.0064
300	80	0.150	0.0072
400	260	0.180	0.0087
500	440	0.211	0.0102
600	620	0.247	0.0119
800	980	0.307	0.0148
900	1160	0.335	0.0161

Density and specific heat of helium is set to zero for transient runs.

4. Air [4]

Temperature	Conductivity	Specific volume	Prandtl No.	Dyn. Visc.
(K)	(W/m-K)	(m^3/kg)	(---)	(Pa-s)
200	0.0180	0.573	0.740	1.33E-05
300	0.0263	0.861	0.708	1.85E-05
400	0.0336	1.148	0.694	2.30E-05
500	0.0403	1.436	0.688	2.70E-05
600	0.0466	1.723	0.690	3.06E-05
800	0.0577	2.298	0.705	3.70E-05
1000	0.0681	2.872	0.707	4.24E-05

Temperature	Conductivity	Density	Prandtl No.	Kin. Visc.
(^{o}F)	(Btu/hr-in-°F)	(lbm/ft^3)	(---)	(ft^2/hr)
-100	0.0009	0.109	0.740	0.2953
80	0.0013	0.073	0.708	0.6172
260	0.0016	0.054	0.694	1.0232
440	0.0019	0.043	0.688	1.5024
620	0.0022	0.036	0.690	2.0430
980	0.0028	0.027	0.705	3.2948
1340	0.0033	0.022	0.707	4.7187

Density and specific heat of air is set to zero for transient runs. Prandtl number, kinematic viscosity, and density of air are used to calculate the convection coefficients in Section 4.9.

5. Solid Neutron Shield (borated Polyester – also used for Polypropylene)

$k = 0.0083$ Btu/hr-in-°F
$c_p = 0.311$ Btu /lb-°F
$\rho = 0.057$ lb/in^3

6. SA-240, Type 304 Stainless Steel (Fuel Compartments, Structural Plates, and Basket Shim)

Temperature (ºF)	Conductivity (Btu/hr-ft-°F) [5]	Conductivity (Btu/hr-in-°F)	Diffusivity [2] (ft^2/hr) [5]	Specific Heat (Btu/lbm-°F)	Density (lbm/in^3) [6]
70	8.6	0.717	0.151	0.117	0.29
100	8.7	0.725	0.152	0.117	
150	9.0	0.750	0.154	0.120	
200	9.3	0.775	0.156	0.122	
250	9.6	0.800	0.158	0.125	
300	9.8	0.817	0.160	0.126	
350	10.1	0.842	0.162	0.128	
400	10.4	0.867	0.165	0.129	
450	10.6	0.883	0.167	0.130	
500	10.9	0.908	0.170	0.131	
550	11.1	0.925	0.172	0.132	
600	11.3	0.942	0.174	0.133	
650	11.6	0.967	0.177	0.134	
700	11.8	0.983	0.179	0.135	
750	12.0	1.000	0.181	0.136	
800	12.2	1.017	0.184	0.136	
950	12.9	1.075	0.191	0.135	
1000	13.2	1.100	0.194	0.136	
1050	13.4	1.117	0.196	0.136	
1100	13.6	1.133	0.198	0.137	
1150	13.8	1.150	0.201	0.137	
1200	14.0	1.167	0.203	0.138	

7. SA 203, Gr. E or SA350, LF3 Steel (Cask Inner Shell, Cask Lid)

Temperature (ºF)	Conductivity (Btu/hr-ft-°F) [5]	Conductivity (Btu/hr-in-°F)	Diffusivity (ft^2/hr) [5]	Specific Heat (Btu/lbm-°F)	Density (lbm/in^3) [6]
70	23.5	1.958	0.458	0.102	0.29
100	23.6	1.967	0.450	0.105	
200	23.6	1.967	0.425	0.111	
300	23.4	1.950	0.401	0.116	
400	23.1	1.925	0.378	0.122	
500	22.7	1.892	0.356	0.127	
600	22.2	1.850	0.336	0.132	
700	21.6	1.800	0.315	0.137	
800	21.0	1.750	0.292	0.144	
900	20.3	1.692	0.269	0.151	
1000	19.7	1.642	0.247	0.159	
1100	19.0	1.583	0.224	0.169	
1200	18.2	1.517	0.200	0.182	
1300	16.9	1.408	0.167	0.202	
1400	15.3	1.275	0.077	0.397	

[2] Thermal diffusivity is $\alpha = \frac{k}{\rho c_P}$, this equation is used to calculate the specific heat.

8. SA 266, Cl. 2 or SA516, Gr. 70 or SA 105 (Carbon Steel)
(Gamma Shield, Cask Outer Shell, Shield Plate, Bottom Plate, and Protective Cover)

Temperature (ºF)	Conductivity (Btu/hr-ft-°F) [5]	Conductivity (Btu/hr-in-°F)	Diffusivity (ft^2/hr) [5]	Specific Heat (Btu/lbm-°F)	Density (lbm/in^3) [6]
70	35.1	2.925	0.695	0.103	0.284
100	34.7	2.892	0.674	0.105	
200	33.6	2.800	0.613	0.112	
300	32.3	2.692	0.561	0.117	
400	30.9	2.575	0.512	0.123	
500	29.5	2.458	0.472	0.127	
600	28.0	2.333	0.433	0.132	
700	26.6	2.217	0.394	0.138	
800	25.2	2.100	0.355	0.145	
900	23.8	1.983	0.317	0.153	
1000	22.4	1.867	0.282	0.162	
1100	20.9	1.742	0.250	0.170	
1200	19.5	1.625	0.218	0.182	
1300	18.0	1.500	0.180	0.204	
1400	16.4	1.367	0.082	0.408	

9. Aluminum Alloy 6061 (Basket Rails, type 1 & 2)

Temperature (ºF)	Conductivity (Btu/hr-ft-°F) [5]	Conductivity (Btu/hr-in-°F)	Diffusivity (ft^2/hr) [5]	Specific Heat (Btu/lbm-°F)	Density (lbm/in^3) [5]
70	96.1	8.008	2.66	0.213	0.098
100	96.9	8.075	2.66	0.215	
150	98.0	8.167	2.65	0.218	
200	99.0	8.250	2.65	0.221	
250	99.8	8.317	2.64	0.223	
300	100.6	8.383	2.63	0.226	
350	101.3	8.442	2.62	0.228	
400	101.9	8.492	2.62	0.230	

10. Aluminum Alloy 6063 (Radial Neutron Shield Boxes)

Temperature (ºF)	Conductivity (Btu/hr-ft-°F) [5]	Conductivity (Btu/hr-in-°F)	Diffusivity (ft^2/hr) [5]	Specific Heat (Btu/lbm-°F)	Density (lbm/in^3) [5]
70	120.8	10.067	3.34	0.214	0.098
100	120.3	10.025	3.30	0.215	
150	119.7	9.975	3.23	0.219	
200	119.1	9.925	3.18	0.221	
250	118.3	9.858	3.13	0.223	
300	118.3	9.858	3.09	0.226	
350	117.9	9.825	3.04	0.229	
400	117.6	9.800	3.00	0.231	

11. Aluminum Alloy 1100 (Paired with Poison Plates, if applicable)

Temperature (ºF)	Conductivity (Btu/hr-ft-°F) [5]	Conductivity (Btu/hr-in-°F)	Diffusivity (ft^2/hr) [5]	Specific Heat (Btu/lbm-°F)	Density (lbm/in^3) [5]
70	133.1	11.092	3.67	0.214	0.098
100	131.8	10.983	3.61	0.216	
150	130.0	10.833	3.50	0.219	
200	128.5	10.708	3.42	0.222	
250	127.3	10.608	3.35	0.224	
300	126.2	10.517	3.28	0.227	
350	125.3	10.442	3.23	0.229	
400	124.5	10.375	3.17	0.232	

12. Poison Plates

The minimum specified conductivity of the poison material is 165 W/m-K (7.94 Btu/hr-in-°F). The conductivity is considered constant (not a function of temperature) for the thermal analysis. The measured conductivities of the available borated aluminum alloys or metal matrix composites are much higher than the above requirement for the entire range of 20°C to 400°C (see Table 9.4-1).

The minimum required thermal conductivities of the paired aluminum and poison plates will be verified via testing as described in Chapter 9.

To minimize the thermal resistance of the basket during the fire period, the conductivity of the poison plate is considered to be equal to the aluminum conductivity. The conductivity of the poison plate is set back to the minimum value of 165 W/m-K (7.94 Btu/hr-in-°F) during the cool down period to maximize the thermal resistance. Specific heat and density of poison plate is set equal to those of aluminum for transient runs.

13. Concrete and Soil (Storage Pad)

The thermal conductivity of normal, saturated concrete varies from 1.2 to 2.0 Btu/ft-hr-°F at temperature ranging from 50 to 150°F [7]. The conductivity of concrete decreases rapidly with the rise in temperature and assumes, at 750°C (1382°F) a conductivity value equal approximately to 50 percent of that of normal temperature [7]. For the thermal analyses a thermal conductivity of 1.15 Btu/hr-ft-°F (0.0958 Btu/hr-in-°F) is considered for concrete at 70°F. This conductivity is reduced by half to a value of 0.0479 Btu/hr-in-°F at 1382°F. A thermal conductivity of 0.3 W/m-K (0.0144 Btu/hr-in-°F) is considered for soil [8].

Since the concrete pad is not present for the transient runs such as the fire accident and the vacuum drying cases, the density and specific heat of concrete and soil are irrelevant for thermal analysis.

14. Emissivities and Absorptivities

The outer surface of the cask is painted white. Reference [9] gives an emissivity between 0.92 to 0.96 and a solar absorptivity between 0.09 and 0.23 for white paints. To account for dust and dirt and to bound the problem, the thermal analysis uses a solar absorptivity of 0.3 and an emissivity of 0.9 for the white painted surfaces.

The emissivity of the cask outer surface is set to 0.8 as required in [11] during the fire burning time. It is assumed that the cask surface is covered with soot after the fire. The solar absorptivity of soot is 0.95 [9]. To bound the problem, the thermal analysis uses a solar absorptivity of 1.0 and an emissivity of 0.9 for cask surfaces during the cool down period.

Emissivity of concrete is reportedly 0.9 to 0.94 [8 & 9]. An emissivity of 0.90 is considered for concrete surfaces. The absorptivity of the concrete surface is 0.73 - 0.91 at 300K [11]. For conservatism a solar absorptivity of 1.0 is considered for concrete surface. These values are used only for the concrete pad during normal/off-normal storage conditions.

4.3 Thermal Evaluation for Normal and Off-Normal Conditions

4.3.1 Thermal Model for Normal and Off-Normal Storage Conditions

The finite element models are developed using the ANSYS computer code [12]. ANSYS is a comprehensive thermal, structural, and fluid flow analysis package. It is a finite element analysis code capable of solving steady-state and transient thermal analysis problems in one, two, and three dimensions. Heat transfer via a combination of conduction, radiation, and convection can be modeled by ANSYS.

A three dimensional, 45 degree symmetric, finite element model is used for evaluation of the normal and off-normal storage conditions. The model includes the full length of the TN-68 cask from the bottom plate to protective cover. A three feet thick concrete pad and seven feet of soil underneath the concrete pad are added to the model to simulate the storage conditions.

In addition to the design basis basket, two alternate design features are evaluated for the TN-68 basket. In the first alternate, the single poison plates are replaced with pairs of poison and aluminum plates. The modeled thickness of the poison plate is 0.1875". The total thickness of the paired poison and aluminum plate is 0.31". In the second alternate, the aluminum and poison paired plates at the periphery of the basket are replaced by aluminum 6061 plates. The geometry of the design basis model is shown in Figure 4.3-1 and Figure 4.3-2. The geometries of the alternate features are shown in Figure 4.3-3. Their performance is compared in Section 4.3.2.

In the TN-68 cask model, the fuel assemblies are considered as a homogenized material within the fuel compartments. The effective properties of the homogenized fuel assemblies are calculated in Section 4.8. The transverse effective fuel conductivity is considered only for the active fuel length region. The active fuel length is considered to be 144" [13] beginning at about 8.0" above the bottom of the fuel assembly [13]. The fuel rod has a total length of about 156" in the model. The conductivity of helium in the transverse direction is considered for the fuel elements beyond the active length. The axial effective fuel conductivity is applied to the total length of the fuel rods.

It is assumed that convection and radiation heat transfers do not occur within cask cavity. Only the effective conductivity calculated for the homogenized fuel includes implicitly the radiation heat transfer. The conduction heat transfer through the basket and cask components is modeled using SOLID70 elements.

The conduction through the protective cover is modeled using SHELL57 elements. For conservatism, no heat transfer is considered between the protective cover and the upper surface of the cask lid to minimize the axial heat transfer, which maximizes the fuel cladding temperature.

The aluminum basket rails are divided into four pieces with an approximate height of 40". A gap of 1/16" is considered between each two adjacent pieces to cover the uncertainties about the quality of the contact between two rail pieces.

Generally, good surface contact is expected between adjacent components within the basket. However, to bound the heat conductance uncertainty between adjacent components, the following gaps are considered in the model at thermal equilibrium:

- 0.01" radial gaps between the neutron shield aluminum boxes and the adjacent shells
- 0.01" axial gap between the cask lid and the cask flange
- 0.01" axial gap between flange of the protective cover and the cask flange
- 0.01" axial gap between the cask lid and the shield plate
- 0.125" axial gap between the bottom plate and the bottom containment
- 0.01" axial gap between the bottom plate and the gamma shield
- 0.01" transverse gap between a poison or aluminum plate and the adjacent stainless steel plate or the fuel compartment wall
- 1/16" axial gap between aluminum rail sections
- 0.125" between the basket and the bottom containment
- 0.10" radial gap between the rails and the cask inner shell[3]
- 0.02" gap between the split aluminum/poison plates only in the basket alternate II

The axial cold gap of 0.07" between the stainless steel structural plates and the poison / aluminum plates is divided into a 0.01" axial gap at the bottom and a 0.06" axial gap at the top of the stainless steel plates. An axial gap of 0.15", equal to the cold gap, is considered between the intersecting poison or aluminum plates.

The inner and outer cask body shells will be assembled with an interference fit. This will assure thermal contact at the shell interface. From Reference [4], the thermal interface conductance increases with contact pressure and reduces with rougher surface finish. At a minimal contact pressure of 5 psi, Reference [4] reports a conductance of 375 Btu/hr-ft^2. For further conservatism, this interface conductance is reduced to 200 Btu/hr-ft^2 for the thermal evaluation. A gap of 0.01" is modeled between the cask inner shell and the gamma shield to simulate the contact resistance of the interference fit. This interference conductance is equal to an effective conductivity of 0.0139 Btu/hr-in-°F for the modeled gap.

$$k_{gap} = 200 \times 0.01\,(\text{in}) / 144\,(\text{ft}^2/\text{in}^2) = 0.0139 \quad \text{Btu/hr-in-°F}$$

4.3.1.1 Steady State Boundary Conditions

The SOLID70 elements representing the homogenized fuel are given heat generating boundary conditions in the region of the active fuel length. A typical axial decay heat profile from measured data (Reference [3]) with a peaking factor of 1.2 is used to distribute the heat in the active fuel region. Section 4.8 describes the methodology and lists the peaking factors used in the model.

The heat generating rate for each segment of the active fuel region is calculated as follows:

[3] The size of the hot gap between the basket rails and the cask inner shell is discussed in Section 4.11.

$$\dot{q}''' = \frac{\left(\frac{q}{a^2 L_a} \times PF\right)}{0.966}$$

where,

q = Decay heat load per assembly (0.441 kW – 1505.4 Btu/hr)
a = Width of the modeled fuel assembly = 6.0”
L_a =Active fuel length = 144”
PF = Peaking Factor from Section 4.9

The area beneath the measured peaking factor curve is 0.996 (see Section 4.9). The heat generating value is divided by this factor to avoid degradation of the total decay heat in the model.

The ambient temperature as a function of time during a peak summer-month day is shown below for a typical site (Reference [2]) with a maximum ambient temperature of 115°F:

Time	12am	2am	4am	6am	8am	10am
Temperature, °F	82	78	75	74	85	97
Time	12pm	2pm	4pm	6pm	8pm	10pm
Temperature, °F	103	111	115	113	100	89

The average temperature over a 24-hour period is 94°F. For conservatism, a maximum daily averaged ambient temperature of 100°F is used for the maximum temperature condition. An ambient temperature of -20°F is considered for the minimum storage conditions.

The free convection and radiation heat transfer to ambient are combined together in form of a total heat transfer coefficient, which is defined as a temperature dependent material property in the model. The total heat transfer coefficients are used to apply the boundary conditions on the outer surface of the cask. Section 4.10 describes the correlations to calculate the total heat transfer coefficients applied on the outer surface of the cask.

Solar radiation is considered as a constant heat flux applied on the SURF152 elements overlaid on the outer surface of the transfer cask. The outer surfaces of the cask are painted white. The insolance values from 10CFR71 [14] are considered as the amount of solar radiation that is available for absorption at any surface. These values are multiplied by the absorptivity factor of each surface to calculate the amount of solar heat flux that each surface absorbs. The resultant value is applied as a constant heat flux to the corresponding SURF152 elements. The heat flux values applied in the model are listed below.

Surface shape	Insolance [14] ($gcal/cm^2$)	Total solar heat flux averaged over 24h ($Btu/hr\text{-}in^2$)	Absorptivity [4]	Solar heat flux in the model ($Btu/hr\text{-}in^2$)
Cask surface, Curved, Painted	400	0.427	0.3	0.128
Cask surface, Flat Horizontal, Painted	800	0.853	0.3	0.256
Concrete, Flat, Horizontal	800	0.853	1.0	0.853

Solar heat flux is not considered for the minimum ambient temperature to maximize the temperature gradient through the cask components.

It is assumed that soil has a temperature of 70°F at 10 feet below the cask bottom plate for hot conditions. The soil temperature for cold condition (-20°F) is assumed to be 45°F. The concrete pad is considered to be 3 feet thick. Due to low conductivity of concrete and soil, the model is insensitive to the thickness of the pad / soil and the soil temperature.

Typical boundary conditions for the transfer cask model are shown in Figure 4.3-4.

4.3.2 Maximum Temperatures for Normal Storage Conditions

Steady state thermal analyses are performed using a total decay heat load of 30 kW (0.441 kW/assembly), 100°F ambient temperature, and the maximum insolation per 10CFR71 [14]. Insolation is averaged over a 24 hour period for the maximum temperature storage conditions.

The resultant temperature distributions for the design basis model are shown in Figure 4.3-5. Figure 4.3-6 shows the temperature distributions in the models with alternate basket types. Summaries of the maximum component temperatures are listed in Table 4.3-1. The resultant temperatures from the design basis model are the bounding values as indicated in Table 4.3-1. Therefore, thermal stresses and cask internal pressures are calculated based on the temperatures resulted from the design basis model.

4.3.3 Minimum Temperatures for Normal Storage Conditions

Temperature distributions under the minimum ambient temperature of $-20^{o}F$ with no insolation and the maximum design heat load of 30 kW are determined under steady state conditions to maximize the temperature gradients in the cask. The design basis model is considered for this evaluation. Table 4.3-2 summarizes the results of this analysis.

4.3.4 Maximum Internal Pressures for Normal Storage Conditions

Maximum internal pressure within the TN-68 cask is calculated in Section 4.7.

[4] See Section 4.2 for discussion

4.3.5 Thermal Stresses for Normal Storage Conditions

Maximum thermal stresses during normal and off-normal storage conditions are calculated in Section 3.4.4. The volumetric average temperatures of the basket, rails, and cask inner shell are retrieved from the thermal model using ANSYS "ETABLE" commands [12] (see Section 4.12 for ANSYS macros). These temperatures are listed in Table 4.3-1 and Table 4.3-2 and used in Appendix 3B.3.4 to calculate the thermal expansion.

4.3.6 Evaluation of Thermal Performance for Normal Storage Conditions

The thermal analysis for storage conditions concludes that the TN-68 design meets all applicable requirements.

The maximum component temperatures calculated using conservative assumptions are lower than the allowable limits. The maximum cask seal temperature (212°F / 100°C) is well below the 536°F long-term limit specified for continued seal function. The maximum radial neutron shield temperature (295°F / 146°C) is below the allowable limits of 300°F (149°C), and the maximum temperature of the top neutron shield (212°F / 100°C) is below the allowable limit of 220°F (104°C). Therefore, no degradation of the solid neutron shielding is expected.

The calculated maximum fuel cladding temperature is 622°F (328°C), which is lower than the temperature limit of 752°F (400°C) considered for normal conditions of storage.

The maximum cask internal pressures for normal and off-normal storage conditions are 18.0 and 21.6 psig respectively. The cask internal pressures are lower than the design pressure of 100 psig.

4.4 Thermal Evaluation for Accident Conditions

The TN-68 casks will be stored on a concrete pad away from combustible material. Therefore, a credible fire would be very small and of short duration such as that due to a fire or explosion from a vehicle or portable crane. However a hypothetical fire accident is evaluated for the TN-68 cask based on a diesel fuel fire, the source of fuel being that from a ruptured fuel tank of the cask transporter tow vehicle. The bounding capacity of the fuel tank is 200 gallons and the bounding hypothetical fire is an engulfing fire around the cask.

Another accident evaluation performed on the cask is the thermal response of the cask in the postulated event of it being completely buried by dirt and debris with very low thermal conductivity. The temperature-time history of the cask components during these events are reported in this section.

4.4.1 Thermal Models for Accident Conditions

The purpose of the accident thermal analyses is to calculate the maximum fuel cladding and the maximum seal temperatures in order to demonstrate the containment integrity of the TN-68 cask. Two models, a cask cross section model and a lid seal region model, are used for the evaluation.

The cask cross-section model is created by selecting the nodes and elements at the midsection of the original cask model described in Section 4.3.1. The selected segment contains all the nodes and elements of the original cask model from z=71.18 to z=83.38 in the axial direction, where the decay heat generation and the resultant temperatures are at their highest for the storage conditions. The height of this model is 12.2", which is equal to the nominal height of one basket segment.

The lid-seal model is created by selecting the nodes and elements at the upper section of the original cask model from z=164.36 to z=204.75 in the axial direction.

The cross-section and the lid-seal models are shown in Figure 4.4-1. The geometry and the material properties of these sub-models are the same as the corresponding locations in the original cask model described in Section 4.3.1.

The initial temperatures for both accident cases are retrieved from the result file of the storage conditions using the sub-modeling ANSYS commands "NWRITE" and "CBDOF" [12]. The boundary conditions for the sub-models are discussed in the following sections.

4.4.1.1 Boundary Conditions for the Hypothetical Fire Accident

An average flame temperature of 1475^{o}F from Reference [14] and a forced convection heat transfer coefficient of 4.5 Btu/hr-ft^{2}-^{o}F from Reference [15] were used for the fire accident case.

From IAEA requirements [16], the "pool" of fuel is assumed to extend 1 meter beyond the cask surface. Based on an outer shell diameter of 98 inches, this gives a "pool" diameter of approximately 176 inches and a pool surface of 24,500 in^2. A fuel consumption rate of 0.15 in/min. was selected from a Sandia Report [15] concerning gasoline/tractor kerosene experimental burning rates. This translates into a fuel consumption rate of approximately 15.9 gal/min. Therefore, the 200 gallons of fuel will sustain a fire for about 13 minutes and hence a 15 minute fire is evaluated.

The forced convection and radiation heat transfer from the fire are combined together as a total heat transfer coefficient. The calculation of the total heat transfer coefficient for fire is discussed in Section 4.10. The total heat transfer coefficients are defined as temperature dependent material properties and used to apply the boundary conditions on the outer surface of the cask. The free convection and radiation during the cool down period are also added together as a total heat transfer coefficient. The calculation of the later coefficient is described in Section 4.10 as well. An ambient temperature of 100°F equal to the maximum storage temperature is considered for the cool down period.

During the cool down period, the solar radiation is applied as a constant heat flux on the SURF152 elements overlaid on the outer surface of the transfer cask. It is assumed that the outer surfaces of the cask are covered with soot after the fire accident. A solar absorptivity of 1.0 (maximum value) is considered for these surfaces to bound the problem. The solar heat flux values applied in the model are listed below.

Surface shape	Insolance [14] ($gcal/cm^2$)	Total solar heat flux averaged over 24h ($Btu/hr\text{-}in^2$)	Absorptivity[6]	Solar heat flux in the model ($Btu/hr\text{-}in^2$)
Cask surface, Curved, Painted	400	0.427	1.0	0.427
Cask surface, Flat Horizontal, Painted	800	0.853	1.0	0.853

For the cross-section model, the heat generating boundary conditions are applied on the elements representing the homogenized fuel with a peaking factor of 1.2. Adiabatic boundary conditions are considered at the both ends of the model.

Although the solid neutron shield might degenerate in the first few minutes of the fire accident, it is assumed that the conductivity of solid neutron absorber remains unchanged during the burning time. For the cool down period the conductivity of solid neutron shield is replaced by air conductivity.

To maximize the heat input from fire into the transfer cask during the burning time, the 0.01” air gaps between the neutron shield aluminum boxes and the adjacent shells are removed and replaced by properties of Al-6063. For the same reason, the shrink fit gap between the inner shell and the gamma shield is also removed during the burning time and replaced by properties of SA 203, Gr. E (cask inner shell). These gaps are put back in place during the cool down

[6] See Section 4.2 for discussion

period to maximize the thermal resistance, which consequently maximizes the fuel cladding temperature.

A minimum conductivity is required for the poison plates. The maximum poison plate conductivity would be lower than that of pure aluminum. The conductivity of the poison plates are increased to the values for aluminum 1100 during the burning time and set back to the minimum required conductivity during the cool down period to bound the uncertainty about the conductivity of poison plates.

To establish the initial temperatures for the lid-seal model, appropriate heat flux values are retrieved from the full cask model and applied on the inner surface of cask lid and on the radial surface of cask inner shell. The locations of heat flux boundary conditions are shown in Figure 4.4-2. A steady state run of the lid-seal model is performed to verify that the applied heat flux values result in the same maximum temperature as concluded from the full cask model.

Radiation heat transfer between the protective cover and the upper surfaces of the cask lid and the top neutron shield is added to the lid-seal model using ANSYS processor "/Aux12" [12]. This radiation transfers the heat from the protective cover at higher temperature caused by the fire to the vent and port cover seals in the cask lid.

The resultant time-temperature histories of the fuel cladding, discussed in Section 4.4.2, show a continuous temperature increase without any extremum for the fire accident case. Therefore, the maximum fuel temperature for the post-fire accident case is calculated using a steady-state run of the cross-section model.

4.4.1.2 Boundary Conditions for the Postulated Buried Cask Accident

All the boundary conditions discussed in Section 4.4.1.1 are also applied for the postulated cask burial case except that adiabatic boundary conditions are considered on the outermost nodes of the cross-section and the lid-seal models.

4.4.2 Maximum Temperatures for Accident Conditions

The time-temperature histories of the cask components are shown in Figure 4.4-3 for the hypothetical fire accident analysis performed on the cross-section and the lid-seal models. As Figure 4.4-3 shows, the fuel cladding temperature increases during the fire and cool down periods without showing any peak. The final temperature distributions resulted from the steady state run of the cross-section model are shown in Figure 4.4-4. The temperature distribution on the lid-seal model is also shown in Figure 4.4-4 at 36 hours after the start of fire. Table 4.4-1 summarizes the maximum temperatures resulted from the transient or the steady state runs for the fire accident case.

Due to adiabatic boundary conditions assumed at the outer surface of the buried cask, the cask component temperatures will only increase for the buried cask accident time. The times at which the component temperatures reach the allowable limits are listed in Table 4.4-2.

4.4.3 Maximum Internal Pressures for Accident Conditions

Maximum internal pressure within the TN-68 cask is calculated in Section 4.7.

4.4.4 Thermal Stresses for Accident Conditions

Maximum thermal stresses during accident conditions are calculated in Section 3.4.4.

4.4.5 Evaluation of Thermal Performance for Accident Conditions

The thermal analysis for the accident conditions concludes that the TN-68 cask meets all applicable requirements.

The maximum fuel cladding temperature is 737°F for the fire accident case as shown in Table 4.4-1. This temperature is well below the allowable limit of 1058°F recommended in [1]. The seal temperatures reach their maximum value at 0.27 hr (16.2 min.) after start of the fire. The maximum seal temperature is 470°F and remains well below the allowable limit of 536°F stated in Section 4.1. It is assumed that the solid neutron shield degenerates during the fire (Section 5.4.7.2). Therefore, the maximum temperature of the solid neutron shield is irrelevant.

The analysis results of the buried cask accident show that if the cask is not uncovered within 0.6 hours, the neutron shield temperature exceeds the allowable limit of 300°F. The fuel temperature exceeds the allowable limit of 1058°F about 90 hours after the cask is buried completely. Seventy six (76) hours after the cask is buried, the average cavity gas temperature reaches 870°F. This temperature corresponds to a cavity internal pressure of 96.7 psig as concluded in Section 4.7. At this moment, the seal temperature remains below the allowable limit of 536°F.

4.5 Thermal Evaluation for Loading and Unloading Conditions

Fuel loading and unloading operations occur in the fuel handling building. During loading operation fuel assemblies are submerged in pool water permitting heat dissipation. After fuel loading is complete, the cask is removed from the pool, drained, sealed, dried, and backfilled with helium.

4.5.1 Vacuum Drying

The loading condition evaluated is the heatup of the cask before the internal pressure of the helium backfilled cask is stabilized at the specified level recommended in [11]. The heatup of the cask occurs typically during the vacuum drying. The vacuum drying process starts after drainage of water to the bottom of the cask cavity.

To determine the time-temperature histories of the cask components during the vacuum drying, transient analyses are performed using the cross-section model of the TN68 cask described in Section 4.4.1. The following material properties are modified in the cross-section model for the analysis of the vacuum drying process:

- The effective conductivity of fuel assemblies is changed to the values calculated for vacuum in Section 4.8
- Air conductivity is given to the elements representing the gas within the cavity

The conductivity of air or helium is independent of the pressure for the conditions considered during the vacuum drying operation. All other material properties remain unchanged. The effective fuel conductivity values used for vacuum conditions are listed in Section 4.2. No convection or radiation is considered within the cask cavity.

The free convection and radiation are combined together to calculate the total heat transfer coefficient from the cask outer surface to the ambient. The correlations to calculate the convection coefficient for vertical plates are discussed in Section 4.10. The following inputs are considered to calculate the total heat transfer coefficient on the radial outer surface of the cask for the cross-section model:

- Ambient temperature in the fuel handling building area is 115°F
- Height of the cylinder is 160”, which is equal to the length of the outer shell
- Surface emissivity of the transfer cask is 0.9 (see Section 4.2)
- View factor from the cask surface to the ambient is 1.0

The decay heat is applied as heat generating boundary conditions on the elements representing the homogenized fuel assemblies with a peaking factor of 1.2. The applied value for the heat generation is:

$$\dot{q}''' = \frac{q}{a^2 L_a} \times 1.2 = 1.02 \qquad \text{Btu/hr-in}^3$$

where,

q = Decay heat load per assembly (0.441 kW / 1505.4 Btu/hr)
a = Width of the modeled fuel assembly = 6.0”
L_a = Active fuel length = 144”

Adiabatic boundary conditions are applied on the top and bottom faces of the cross-section model for conservatism.

An average, initial temperature at the beginning of the transient run is calculated for the cask as follows.

Initial Temperature = initial pool temperature +
average heatup rate with water in cask cavity × duration of lifting +
average heatup rate without water in cask cavity × duration of drainage

Following assumptions are considered to calculate the initial temperature.

- Initial pool temperature is 125°F
- No convection and radiation heat dissipation occur from the cask outer surface
- All the decay heat is used to heat up the cask and its content

Specific heat values increase generally at higher temperatures. Specific heats of the components are taken at about 100°F, which results in higher initial temperature and increases the conservatism in the model. The average heat up rate is:

$$heat\ up\ rate = \frac{Q}{\sum M\,C_p}$$

Q = total decay heat load = 30 kW (102,369 Btu/hr)
M = component weight (lbm)
C_p = specific heat (Btu/lbm-°F)

The components volumes and weights are taken from Chapter 3. A summary of the heat up rate calculation is shown in Table 4.5-1.

It is considered that lifting the cask from the pool to the decontamination area and performing the required inspections takes 2 hours. The water in the cask can be pumped out with a rate of 6 to 10 gal/min. Table 4.5-1 gives the total amount of water in the cask cavity. Assuming a pump rate of 6 gal/min, it takes less than five hours to drain the water from the cavity completely. The initial average temperature of the cask and its content is then:

Initial average temperature = 125 + 2.7 × 2 + 4.2 × 5 = 152°F
with initial pool temperature =125°F
average heat up rate during lifting = 2.8°F /hr (see Table 4.5-1)
duration of lifting = 2 hrs
average heat up rate after drainage of cask cavity = 4.3 °F /hr (see Table 4.5-1)
duration of cask water draining = 5 hrs

An initial temperature of 160°F is considered for the cask and its contents at the start of the transient runs.

The transient analysis of the vacuum drying procedure gives the time-temperature histories of the fuel assemblies with a maximum decay heat load of 30 kW. Duration of the vacuum process is limited to the time at which the maximum temperature of the fuel assemblies is equal to the allowable limit of 752°F (400°C).

Should the decay heat load be lower than 30 kW, the time for reaching this limit will increase. At a certain decay heat load, the maximum fuel cladding temperature remains always below the allowable limit regardless of the vacuum drying duration. To determine the decay heat load at which no time limit is required for the vacuum drying, a steady state analysis is performed on the full cask model described in Section 4.3.1. This model is modified for the purpose of the analysis. The modifications are as follows:

- Cask protective cover, concrete pad, and soil are removed from the model
- Adiabatic boundary conditions are considered at the bottom of the cask
- Free convection and radiation to 115°F ambient are applied at the upper surface of the cask lid
- A view factor of 1.0 is considered for all the cask outer surfaces
- Insolance is not considered in the model
- Effective fuel conductivities are changed to those calculated for vacuum conditions
- Gasous conductivity of air is considered for the gaps within the basket

The other material properties and boundary conditions are the same as those described in Section 4.3.1.

In addition to the above cases, it is assumed that the cask with 30 kW heat load would be backfilled with helium no more than 30 hours after drainage of the water from the cask cavity. This helium backfill could be either the backfill after successful demonstration of dryness, or an intermediate backfill, after which vacuum drying is resumed. A transient run is performed using the cross-section model of TN68 cask to analyze this case. The effective fuel conductivity and the conductivity of gas within the basket gaps are changed from air to helium in this model after the intermediate helium backfilling occurs.

The maximum component temperatures after backfilling with helium are determined using a steady state run of the full cask model with the boundary conditions outlined above.

Similar to Section 4.3.5, the volumetric average temperatures of the basket, rails, and cask inner shell are retrieved from the thermal model to calculate the thermal expansion in Appendix 3B. A zero gap at thermal equilibrium is assumed between the rails and the cask inner shell in retrieving the average temperatures. These temperatures are listed in Table 4.5-2.

4.5.1.1 Evaluation of Vacuum Drying Procedure

The time-maximum temperature histories of selected components are collected in Figure 4.5-1 for vacuum drying with 30 kW decay heat load, and a 0.10 inch hot gap between the basket and the cask. The fuel cladding and the radial neutron shielding material are subject to temperature limits which are not exceeded at 37 hours as shown in Table 4.5-2.

The allowable time for vacuum drying increases for lower decay heat loads. A steady state analysis of the vacuum drying shows that the fuel cladding temperature remains always below the allowable limit of 752°F when the decay heat load is equal or less than 25.25 kW. The radial neutron shielding temperature also remains below its limit under this condition as shown in Table 4.5-2.

The time-temperature history for the vacuum drying procedure with 30 kW heat load and with helium backfilling at 30 hours is shown in Figure 4.5-1b. The fuel cladding temperature history in Figure 4.5-1b shows that the fuel cladding temperature drops immediately after backfilling with helium and reaches eventually the temperature determined in a steady state analysis, 596°F, well below the allowable limit of 752°F. The results are summarized in Table 4.5-3.

Once helium is introduced, subsequent evacuation and backfilling with helium will not change the conductivity of the cavity gas, and therefore no cycling of the fuel cladding temperature occurs.

The conclusion is that in order to maintain the fuel cladding temperature below the 752°F for a load above 25.25 kW, vacuum drying must be completed within 37 hours, or helium must be introduced at or before 37 hours. At or below 25.25 kW, there need be no vacuum drying time limit for the purpose of limiting cladding temperature.

Similar to Section 4.3.5, the volumetric average temperatures of the basket, rails, and cask inner shell are retrieved from the cross-section thermal model to calculate the thermal expansion. The temperatures correspond to Figure 4.5-1(b) at 30 hours prior to helium backfilling. These temperatures assume there is a radial gap at the hot condition. To maintain average temperatures at or below these under vacuum in the steady state, the decay heat load must be 22 kW or less.

If the basket were to expand until that radial gap closed, the basket temperatures would then decrease while the cask temperatures would continue to increase. This condition is evaluated using temperatures at 30 hours and 30 kW load with a zero gap between the rails and the cask inner shell, modeled by increasing the conductivity of the perimeter elements.

The temperatures for thermal expansion evaluation (Appendix 3.B.3.4) are listed in Table 4.5-2.

4.5.2 Reflooding

For unloading operations, the cask will be filled with the spent fuel pool water through the drain port. During this filling, the cask vent port is maintained open with effluents routed to the plant's off-gas monitoring system.

When the pool water is added to a cask cavity containing hot fuel and basket components, some of the water might flash to steam causing internal cavity pressure to rise. The steam pressure is released through the vent port. The initial flow rate of the reflood water must be controlled such that the internal pressure in the cask cavity stays below the design pressure of 100 psig. In the event that the cask internal pressure increases to 75.3 psig (90 psia), the check valve shuts off the flow of water into the cask preventing the pressure from increasing. See the unloading operations in Section 8.2.

A quench analysis of the fuel is performed in Section 3.5.2 and concludes that the total stress on the cladding as a result of this operation is below the cladding material's minimum yield stress.

4.6 Thermal Evaluation of TN-68 Cask Containing Damaged Fuel

Maximum 8 damaged fuel assemblies can be stored in the basket of the TN-68 cask. Damaged fuel is defined in Section 2.1. Location of the damaged fuel assemblies considered in this analysis is shown in Figure 4.6-1.

The finite element model developed in Section 4.3.1 is considered to evaluate the effects of the damaged fuel assemblies on the thermal performance of TN-68 cask. The modification of this model and the boundary conditions are discussed in the following sections.

4.6.1 Normal Storage Conditions

The structural analysis in Appendix 6B demonstrates that under normal conditions, the geometric form of the damaged fuel will not be substantially altered. However, the thermal analysis considers a reduction of the damaged fuel conductivity in both the axial and the transverse direction to bound the thermal effects. The effective conductivities of damaged fuel assemblies are discussed in Section 4.8. The finite element model for the normal and off-normal storage conditions is modified to consider the effective properties of damaged fuel assemblies for the damaged fuel regions shown in Figure 4.6-1.

All other material properties and boundary conditions remain the same as those in described in Section 4.3.1. Particularly, identical decay heat profiles are considered for both the damaged and the intact fuel assemblies for this analysis. The total decay heat load is 30kW.

4.6.2 Accident Conditions

To bound the thermal effect, it is assumed that the cladding of the damaged fuel assemblies breaks entirely in consequence of a drop accident. In that event, the fuel pellets would be released in the compartment space. The end caps will hold the fuel rubble within the compartment volume. The concentration of the decay heat for the fuel rubble is maximized, when all the rubble is compressed to a minimum height at one end of the fuel compartment. To bound the maximum cladding temperature of the intact fuels, it is assumed that all the 8 damaged fuel assemblies transform to rubble. To minimize the volume, the cladding is assumed to fill all the space between intact pellets. An approximate void volume between the pellets can be evaluated considering the area ratio of a pellet cross-section (circle with diameter D) to a surrounding square with the same cutout D. The ratio of the void volume to the pellet volume is:

$$\frac{V_{void}}{V_{UO_2}} = \frac{A_{square} - A_{pellet}}{A_{pellet}} = \frac{D^2 - \frac{\pi}{4}D^2}{\frac{\pi}{4}D^2} = \frac{4}{\pi} - 1 = 0.27$$

The minimum height of the fuel rubble is calculated as follows.

$$H_{\min} = \frac{V_{UO2} \times 1.27 + V_{Zr4}}{A}$$

where

A = cross-sectional area of the fuel compartment = $6.0 \times 6.0 = 75.69$ in^2
V_{UO2} = volume of fuel pellets
V_{Zr4} = volume of fuel cladding

Table 4.6-1 summarizes the calculation of H_{min} for all the fuel types. The shortest height shown of the fuel rubble is 54". The finite element model of the TN-68 cask is modified to consider the shortest fuel rubble height. The decay heat load is applied to the fuel rubble as a uniform heat generation rate without peaking factor.

$$\dot{q}'''_{rubble} = \frac{q}{a \times a \times H_{\min}} = 0.77 \qquad \text{Btu/hr - in}^3$$

where

q = decay heat per assembly = 0.441 kW/assembly (1505.4 Btu/hr-assembly)
a = fuel compartment size = 6"
H_{min}= 54" (see Table 4.6-1)

Thermal properties of helium are considered for the elements representing the fuel rubble to eliminate the uncertainties regarding the fuel rubble conductivity. The decay heat profile from Section 4.9 is considered for the intact fuels for this analysis. The total decay heat load remains 30kW.

The cask drop accident could occur before or after the fire accident. Section 4.4.2 shows that for the accident conditions, the maximum fuel cladding temperature will be reached at the steady state run cooldown conditions. Therefore, the cooldown boundary conditions in a steady state run are considered for the TN-68 cask model containing fuel rubble to determine the bounding fuel cladding temperature for the accident conditions.

Except for those mentioned above, the geometry and material properties of all other elements in the TN-68 cask model remain unchanged.

4.6.3 Evaluation of the Thermal Performance with Damaged Fuel

To establish the heat removal capability and the integrity of the intact fuel cladding, maximum fuel cladding temperature limits of 752°F and 1058°F are considered for normal storage and accident conditions respectively. These limits are based on NRC recommendations [1].

The maximum temperatures for a cask containing 8 damaged fuel assemblies are shown in Table 4.6-2 for the normal storage conditions. A comparison between the temperatures in Table 4.6-2 and Table 4.3-1 shows that the maximum fuel cladding temperature remains unchanged for the

cask containing 8 damaged fuel assemblies under normal storage conditions. The basket component temperatures change only by ±1°F for this case. Regarding the margin to the allowable limit these temperature changes are insignificant. Therefore, the cask cavity pressure remains also unchanged.

Table 4.6-3 shows the resultant temperatures for the accident case. A comparison between the maximum component temperatures in Table 4.6-3 and the corresponding values in Table 4.4-1 for a cask containing 68 intact fuel assemblies shows that the maximum temperatures decreases significantly when the damaged fuel assemblies are transformed to rubble in the consequence of an accident. The average cavity gas pressure remains therefore bounded by the values calculated for the accident case of a cask containing 68 intact fuel assemblies.

Handling and Storage of 8 damaged fuel assemblies in the TN-68 cask does not alter the thermal performance and all the temperatures remain below the allowable limits for normal and accident conditions.

4.7 Maximum Internal Pressure

The following methodology is used to determine the maximum pressures within the TN-68 cask cavity for normal, off-normal, and accident conditions:

- Average cavity gas temperatures are derived from the TN-68 thermal models.
- The amount of helium present within the cask cavity after the initial backfilling is determined via the ideal gas law.
- The total amount of free gas within the fuel assemblies, including both fill and fission gases, are calculated based on NUREG 1536 [11] recommendations.
- The amount of released gas from the fuel rods into the cask cavity is determined based on the maximum fraction of the ruptured fuel rods considered in NUREG 1536 [11].
- The amount of helium backfill gas is added to the amount of released gases to make the total amount of gases in the cask cavity.
- Finally, the maximum cask internal pressures are determined via the ideal gas law.

A maximum absolute pressure of 2.2 atm is considered for the initial backfill pressure to maintain the helium pressure in the cavity for a long storage period. The design pressure for the TN-68 cask is 100 psig per Table 2.5-1.

To bound the maximum internal pressure, the maximum ambient temperature of 100°F is considered for both normal and off-normal conditions.

As it is assumed in NUREG 1536 [11], the maximum fractions of the fuel rods (f_B) that can rupture and release their free gases to the cask cavity for normal, off-normal, and accident conditions are 1, 10, and 100% respectively.

4.7.1 Average Gas Temperature

To determine the average gas temperature, volume average temperatures of the elements representing the helium gaps ($T_{avg,void}$) and the homogenized fuel assemblies ($T_{avg,fuel}$) are retrieved from the thermal models using the ETABLE commands in ANSYS [12] (See Section 4.12 for ANSYS macros). Although the average temperature of the homogenized fuel elements includes the fuel rods and the helium gas between them, this average temperature is considered as the average gas temperature within the fuel compartments. The following volumes are considered to calculate the gas average temperature:

Gas volume in fuel compartments = Volume of fuel compartment – Volume of fuel rods
Volume of fuel compartments = $6 \times 6 \times 164 \times 68 = 401{,}472$ in^3
Volume of fuel assemblies = 158,267 in^3
Gas volume in fuel compartments ($V_{gas,comp}$) = 243,205 in^3

The volume of the gas in the void space of the cask cavity is:

Gas volume in void space of cask = Total cask cavity volume – Gas volume in fuel compartments

Total cask cavity volume (V_{cavity}) loaded = 365,574 in^3

Gas volume in fuel compartments = 243,205 in^3

Gas volume in void space of cask (V_{void}) = 122,369 in^3

The average gas temperature in the cask cavity is calculated as follows.

$$\overline{T}_{Cavity} = \frac{T_{avg,fuel} \times V_{gas,comp} + T_{avg,void} \times V_{void}}{V_{cavity}}$$

The results are summarized below.

Operating Condition	$\overline{T}_{Cavity}$ (°F)
Normal (Off-Normal) Storage Conditions	402
Fire Accident	572
Buried Cask Accident, 76 hrs after occurrence	870

4.7.2 Amount of Initial Helium Backfill

An equilibrium cask cavity pressure of 2.2 atm abs is considered for the initial normal storage conditions. The amount of the helium backfill gas at this moment is calculated based on the cavity gas temperature for the normal storage conditions using the ideal gas law as follows.

$n_{back} = (P_{st}\ V)/(RT_{st})$

P_{st} = equilibrium cask cavity pressure (normal storage) = 2.2 atm = 32.3 psia

V = cask cavity volume (loaded) = 365,574 in^3 = 211.6 ft^3

T_{st} = equilibrium storage temperature = 402°F = 862 R

R = universal gas constant = 10.730 psia-ft^3/lbmol-R

n_{back} = 0.74 lbmol

4.7.3 Free Gas within Fuel Assemblies

The maximum amount of fission gas per assembly is 1.57×10^{-2} kgmol/assembly as concluded in Section 5.2.4. The amount of fill gas for each assembly type to be stored in TN-68 cask is calculated as follows using the data from Table 5.2-1.

$n_{fill} = (P_i\ V_{free})/(RT)$

P_i = initial rod pressure (psia)

T = initial fill temperature = 0°C = 273K

V_{free} = Annulus volume + Plenum volume

Annulus volume = $L_a \times \pi/4\ (ID_{rod}^2 - OD_{pellet}^2)$

Plenum volume = $L_{plenum} \times \pi/4 \, (ID_{rod}^2)$
L_a = active fuel length

To calculate the total amount of free gas in the cavity, it is assumed that 30% of the fission gases and 100% of the fill gas will be released from ruptured fuel rods into the cask cavity, as required in [11]. The following table summarizes the results.

Fuel Type	Fill Gas (kgmole/rod)	No. of Rods	Fill Gas (kgmole/assembly)	Fission Gas (kgmole/assembly)	Total Free gas (kgmole/assembly)
GE4 (8x8-63/1)	3.842E-06	63	2.420E-04	1.57E-02	4.952E-03
GE8, type II (8x8-62/2)	8.176E-06	62	5.069E-04	1.57E-02	5.217E-03
GE9, GE10 (8x8-60/4)	8.177E-06	60	4.906E-04	1.57E-02	5.201E-03
GE11, GE12 (8x8-60/1)	8.247E-06	60	4.948E-04	1.57E-02	5.205E-03
GE11, GE13 (9x9-74/2)	1.800E-05	74	1.332E-03	1.57E-02	6.042E-03
GE12 (10x10-92/2)	1.492E-05	92	1.373E-03	1.57E-02	6.083E-03
Max					**6.083E-03**

As the above table shows, the maximum of the free gas is bounded by 6.083×10^{-3} kgmol/assembly. The total amount of free gas in the cask cavity is:

$n_{free} = 6.083 \times 10^{-3} \times 68 = 0.41$ kgmol = 0.91 lbmol

4.7.4 Total Amount of Gases within Cask Cavity

The total amount of gases within the cask cavity is equal to the amount of the initial helium backfill gas plus any free gases that are released to the cask cavity from ruptured fuel rods.

Total amount of gases in the cask cavity are:
$n_{total} = n_{back} + f_B \, (n_{free})$

n_{total} = total amount of gases	lbmol
n_{back} = total amount of backfill gas = 0.74	lbmol
n_{free} = total amount of free gases = 0.91	lbmol
f_B = fraction of the ruptured fuel rods	(NUREG-1536 [11])

4.7.5 Maximum Cask Internal Pressure

The maximum internal cask internal pressure (P_{cavity}) is determined via the ideal gas law:

$P_{cavity} = (n_{total} R \overline{T}_{cavity})/V$

P_{cavity} = Internal cavity pressure (psia)
V = Cavity volume (loaded) =365,574 in^3 = 211.6 (ft^3)
R = universal gas constant = 10.73 (psia-ft^3/lbmol-°R)

The results are summarized in the following table.

	n_{back}	f_B [4.1]	n_{free}	n_{total}	$\overline{T}_{cavity}$	P_{cavity}	P_{cavity}
Operating Condition	(lbmol)	(---)	(lbmol)	(lbmol)	(°F)	(psia)	(psig)
Normal equilibrium, no ruptured fuel							17.6
Normal Storage	0.74	0.01	0.91	0.75	402	32.7	18.0
Off-Normal Storage	0.74	0.10	0.91	0.83	402	36.3	21.6
Fire Accident	0.74	1.0	0.91	1.65	572	86.4	71.7
Buried Cask Accident, 76 hrs after occurrence	0.74	1.0	0.91	1.65	870	111.4	96.7

The internal cask cavity pressures are below the design limit of 100 psig.

4.8 Effective Fuel Properties

4.8.1 Discussion

The finite element models of the TN-68 cask simulate the effective thermal properties of the fuel with a homogenized material occupying the volume within the basket where the fuel assemblies are stored. Effective values for density, specific heat, and conductivity are determined for this homogenized material for use in the finite element models.

The TN-68 cask is capable of handling a variety of intact and damaged spent BWR fuel assemblies. In order to determine conservative thermal properties of the homogenized fuel assembly, all of the BWR fuel assembly types to be stored in the TN-68 cask are studied. The lowest effective thermal conductivity, density, and specific heat of the studied fuel assemblies are selected to apply in the finite element model. Use of these properties would conservatively predict bounding maximum temperatures for the components of the TN-68 cask.

In order to bound the effect that damaged fuel might have, the effective thermal properties of damaged fuel are calculated assuming changes in fuel rod pitch and rupture of fuel rods.

The characteristics of the fuel assemblies to be stored in the TN-68 cask are listed in Table 5.2-1. A channel internal width of 5.278" is considered for all fuel assembly types. The methodology to calculate the effective fuel properties are described in Sections 4.8.3 and 4.8.4. The results are discussed in Section 4.8.5.

4.8.2 Summary of Material Properties

The following properties are considered for UO_2 and Zircaloy for calculation of the effective fuel properties.

	k	Cp	ρ	Emissivity
Material	**(Btu/hr-in-°F)**	**(Btu/lbm-°F)**	**(lbm/in^3)**	**(---)**
UO_2	0.1926 [17]	0.0560 [18]	0.396 [18]	---
Zircaloy	0.6019 [17]	0.0657 [17]	0.237 [18]	0.74 [17]

The conductivities of helium and air as backfill gas are listed in Section 4.2. The air conductivity is used for vacuum drying conditions. The vacuum drying process generally does not reduce the pressure sufficiently to reduce the thermal conductivity of the water vapor and air in the cask cavity. Therefore, air conductivity is assumed for the backfill gas for vacuum drying conditions and the effect of water vapor conductivity is neglected for conservatism. For other conditions, the conductivity of helium is used for backfill gas.

The measured emissivity of stainless steel is 0.46 [10]. For conservatism, an emissivity of 0.2 is considered for the fuel compartments in calculation of the transverse effective fuel conductivity.

4.8.3 Effective Fuel Conductivity

4.8.3.1 Transverse Effective Conductivity for Intact Fuel

The purpose of the effective conductivity in the transverse direction of a fuel assembly is to relate the temperature drop of a homogeneous heat generating square to the temperature drop across an actual assembly cross section for a given heat load. This relationship is established by the following equation obtained from Reference [19]:

$$k_{eff} = \frac{q}{4L_a(T_c - T_o)}(0.29468) = \frac{q_{react}}{4(T_c - T_o)}(0.29468)$$

where:

k_{eff} = Effective thermal conductivity (Btu/hr-in-ºF)
q = Assembly head generation (Btu/hr)
q_{react} = Reaction solution retrieved from the 2D model (Btu/hr)

$$q = q_{react} \times L_a$$

L_a = Assembly active length (in)
T_o = Maximum temperature (ºF)
T_s = Surface temperature (ºF)

The methodology to calculate the transverse effective conductivity for BWR fuel assemblies is discussed in detail in Reference [20]. In this methodology, two dimensional finite element models of each fuel assembly type is developed using the ANSYS computer code [12]. The two-dimensional models simulate the heat transfer by radiation and conduction and include the geometry of the fuel rods, fuel pellets, and channels. The channel is included for transverse effective conductivity because it reduces radiative heat transfer between the fuel rods and compartment walls. All components are modeled using 2D PLANE55 thermal solid elements. Radiation between the fuel rods and the channel and between the channel and the compartment walls is simulated using the /AUX12 processor in ANSYS. For this purpose, LINK32 elements are placed on the exteriors of the fuel rods for creation of the radiation super-element. The compartment walls are also modeled using LINK32 elements and used only to set up the surrounding surface for the creation of the radiation super-element (MATRIX50). All LINK32 elements are unselected prior to solution of the thermal problem. Helium conductivity is considered for the fill gas in the fuel assembly. The other thermal properties used in the model are described in Section 4.8.2.

A fuel assembly decay heat load of 0.264 kW [8] is used for heat generation. An active length of 144" is assumed for the model. Several computational runs were made for each fuel type model using isothermal boundary temperatures ranging from 100 to 600ºF. The isothermal boundary conditions are applied on the outermost nodes of the model, which represent the compartment walls. In determining the temperature dependent effective conductivities of the fuel assemblies an average temperature, equal to $(T_o + T_s)/2$, is used for the fuel temperature. The finite element

[8] Although 0.264 kW is lower than the design decay heat load of 0.441 kW per assembly, it is adequate to determine the fuel assembly type with the minimum transverse conductivity.

models are used to calculate the maximum temperature difference between the center of the fuel assembly and the isothermal boundary conditions.

The results of this study shown in Figure 4.8-1 determine that the fuel assembly GE4 (8x8-63/1) has the lowest transverse effective conductivity for temperatures above 400°F. The analysis of the effective transverse conductivity is repeated for GE4 (8x8-63/1) with 0.441 kW decay heat load and exterior wall temperatures from 100 to 1100°F to cover the entire range of the expected temperatures. The transverse effective conductivity is calculated with helium as backfill gas for normal and accident storage conditions. For vacuum drying conditions, the conductivity of helium is replaced by air conductivity.

4.8.3.2 Transverse Effective Conductivity for Damaged Fuel

To determine the effect that damaged fuel might have on effective transverse conductivity, it is assumed that the fuel rods in a damaged assembly could move in axial and in transverse directions. The axial movement of the fuel rods has no impact on the thermal conductivity in either direction. However, the transverse movement of the rods affects the transverse fuel conductivity.

The study of intact fuel assemblies in Reference [20] shows that the intact fuel assembly GE2 (7x7-49/0) has the lowest transverse conductivity under 400ºF and the intact fuel assembly GE4 (8x8-63/1) has the lowest transverse conductivity over 400ºF. Therefore, the impact of the transverse movement on the fuel effective conductivity is determined using the characteristics of GE2 and GE4 fuel assemblies.

The effect of the transverse moving of the fuel rods is investigated by changing the pitch size of the fuel rods from the minimum closest packed pitch to the maximum most spread out pitch using two dimensional ANSYS models. These models are created in the same way as described in Section 4.8.3.1. A minimum gap of 0.01" is considered between the fuel rods for the minimum pitch size and between the fuel rods and the compartment walls for the maximum pitch size. The models are run with various isothermal boundary conditions for each pitch size. The effective transverse fuel conductivity is determined using the same equation described in Section 4.8.3.1.

The investigation shows that the reconfigured fuel assembly GE2 provides the lowest transverse conductivities at a pitch size of 0.607". The resultant minimum transverse effective conductivities for reconfigured fuel under helium atmosphere are discussed in Section 4.8.5.

Reconfiguration of the fuel rods as a consequence of damaged grids does not have any impact on the other effective fuel properties such as density, specific heat, and axial conductivity.

4.8.3.3 Axial Effective Conductivity

The backfill gas, fuel pellets, and Zircaloy behave like resistors in parallel. However, due to the small conductivity of the fill gas and the axial gaps between fuel pellets, credit is only taken for the Zircaloy fuel rods in the determination of the axial effective conductivities. Water rods and channel are neglected.

$$k_{eff,axl} = \frac{cladding\ area}{a^2} \times k_{Zr} = \frac{A_{zr}(in^2)}{6 \times 6} \times 0.6019 \qquad \text{(Btu/hr-in-°F)}$$

To consider the reduction in axial conductivity of damaged fuel, the axial effective conductivity of the intact fuel is decreased by 10% for the elements representing the damaged fuel assemblies in the model.

4.8.4 Effective Fuel Density and Specific Heat

Volume average density and weight average specific heat are calculated to determine the effective density and specific heat for each intact fuel assembly type separately. The equations to determine the effective density and specific heat are shown below.

$$\rho_{eff} = \frac{\sum \rho_i V_i}{V_{assembly}} = \frac{\rho_{UO_2}\ V_{UO_2} + \rho_{Zr}\ V_{Zr}}{a^2 L_a}$$

$$C_{p,eff} = \frac{\sum m_i\, C_{Pi}}{\sum m_i} = \frac{M_{UO_2}\, C_{P,UO_2} + M_{Zr}\, C_{P,Zr}}{M_{UO_2} + M_{Zr}}$$

The thermal performance of the cask containing damaged fuel is evaluated using steady state conditions. Therefore, calculation of density and specific heat is irrelevant for damaged fuel assemblies.

4.8.5 Conclusion

The calculated transverse effective conductivities of intact GE4 (8x8/63/1) fuel assembly with helium backfill gas for storage and with air backfill gas for vacuum drying conditions are listed in Table 4.8-1.

The axial effective conductivity, effective density, and effective specific heat for each fuel type are calculated using the equation from Sections 4.8.3.3 and 4.8.4. The resultant values are listed in Table 4.8-1.

The lowest axial effective conductivity belongs to GE11 (9x9 – 74/2) fuel assembly, which is used in the thermal model.

Since using the lowest density and specific heat result in the highest cladding temperature for accident conditions, the density of fuel assembly GE8, type II (8x8 – 60/4), and the specific heat of GE9 (8x8 – 60/1) are selected as bounding values to use in the thermal models.

The calculated transverse effective conductivity for reconfigured fuel assembly GE2 (7x7-49/0), as well as the reduced axial effective conductivity are listed in Table 4.8-2.

4.9 Axial Decay Heat Profile

The typical axial decay heat profile is based on the measured data from Reference [3]. These data are listed below.

% of Core Height	Corresponding Length from Bottom of Active Fuel (in)	Peaking Factor	Area under the Profile
0.0%	0.00	0.00	0.00
2.0%	2.88	0.20	0.29
6.0%	8.64	0.71	2.62
8.5%	12.24	0.86	2.83
10.0%	14.40	0.96	1.97
14.5%	20.88	1.09	6.64
16.9%	24.34	1.12	3.82
18.9%	27.22	1.14	3.25
22.5%	32.40	1.18	6.01
25.4%	36.58	1.18	4.93
25.5%	36.72	1.18	0.17
30.5%	43.92	1.20	8.57
33.8%	48.67	1.20	5.70
34.5%	49.68	1.20	1.21
37.5%	54.00	1.20	5.18
42.0%	60.48	1.20	7.78
42.3%	60.91	1.20	0.52
46.0%	66.24	1.20	6.39
50.0%	72.00	1.20	6.91
50.7%	73.01	1.20	1.21
54.0%	77.76	1.20	5.70
58.0%	83.52	1.19	6.88
59.2%	85.25	1.18	2.05
62.0%	89.28	1.17	4.74
65.5%	94.32	1.15	5.85
67.6%	97.34	1.14	3.46
69.5%	100.08	1.13	3.11
74.5%	107.28	1.08	7.96
76.1%	109.58	1.07	2.48
78.5%	113.04	1.06	3.68
81.5%	117.36	1.00	4.45
84.5%	121.68	0.92	4.15
85.5%	123.12	0.90	1.31
90.0%	129.60	0.75	5.35
94.0%	135.36	0.56	3.77
98.0%	141.12	0.20	2.19
100.0%	144.00	0	0.29
SUM			143.40
Average			**0.996**

The average value in the above table is the total area under the axial decay heat profile divided by the active fuel length. This value must be equal to 1. Since it differs from one, a correction factor of 1/0.996 is multiplied by the heat generating rate to avoid any degradation of the applied heat in the model.

An active fuel length of 144" is considered for the bounding fuel assembly. Twenty seven axial fuel regions are defined for the fuel assembly in the finite element model. An average peaking factor is calculated for each region so that the resultant axial profile is identical to the profile from the above table.

The average peaking factor of each fuel region is set equal to the area underneath the peaking factor curve divided by the height of the corresponding region. The area underneath the peaking factor curve is calculated as follows.

$$A_j = \sum_{1}^{n} \frac{(P_{i+1} + P_i)}{2(l_{i+1} - l_i)}$$

where,

A_j = area underneath the profile in fuel region j
P_i = Local peaking factors at location i in fuel region j
l_i= Corresponding length to the local peaking factor P_i

The average peaking factor is:

$$P_j = \frac{A_j}{H_j}$$

P_j = Average peaking factors of fuel region j
H_j= Height of fuel region i

The following Figure depicts this methodology.

Calculation of the Average Peaking Factor

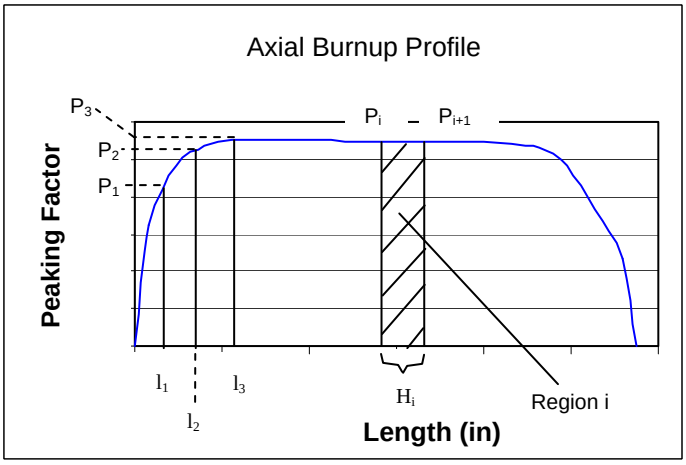

The resultant average peaking factors for active fuel length of 144" are listed in Table 4.9-1. The height of each region is converted to the corresponding local coordination in the finite element model to apply the peaking factors in the model. The peaking factors applied in the model are listed in Table 4.9-2. A comparison between the measured axial decay heat profile and the one used in the finite element model is shown in Figure 4.9-1.

4.10 Heat Transfer Coefficients

4.10.1 Total heat Transfer Coefficient to Ambient (Free Convection)

The outer surfaces of the cask dissipate heat to the ambient via free convection and radiation. Total heat transfer coefficient is defined as:

$$H_t = h_r + h_c \qquad \text{Eq. 4.10-1}$$

where,

h_r = radiation heat transfer coefficient
h_c = free convection heat transfer coefficient

The radiation heat transfer coefficient, h_r, is given by the equation:

$$h_r = \varepsilon F_{12}\left[\frac{\sigma\left(T_1^{\,2} - T_2^{\,2}\right)}{T_1 - T_2}\right] \quad \text{(Btu/hr-ft}^2\text{-°F)} \qquad \text{Eq. 4.10-2}$$

where,

ε = surface emissivity
F_{12} = view factor from surface 1 to ambient
$\sigma = 0.1714 \times 10^{-8}$ Btu/hr-ft^2-°R^4
T_1 = surface temperature, °R
T_2 = ambient temperature, °R

Since the TN-68 casks may be stored in two $2 \times \infty$ arrays separated by about 30 ft and a pitch of 14 ft as shown in Figure 4.10-1, the radiation view factor from the radial cask surfaces to the environment is less than 1.0. This view factor is calculated as follows.

Reference [4], view factor configuration number 4, calculates the view factor between a cylinder and a finite plane of the same height as follows:

a = Distance between cylinder centerline and plane
b = Width of plane
c = Height of plane and cylinder
d = Radius of cylinder
X = a/d, Y = b/d, Z = c/d
$A = Z^2 + X^2 + E^2 - 1$, $B = Z^2 - X^2 - E^2 + 1$

$$F_{Cylinder-Plane} = \frac{2}{Y}\int_0^{Y/2} f(E)\,dE \qquad \text{Eq. 4.10-3}$$

$$f(E) = \frac{X}{X^2 + E^2} - \frac{X}{\pi(X^2 + E^2)}\left\{\cos^{-1}\frac{B}{A} - \frac{1}{2Z}\left[\begin{array}{l}\sqrt{A^2 + 4Z^2}\cos^{-1}\left(\dfrac{B}{A\sqrt{X^2 + E^2}}\right) + \\ B\sin^{-1}\left(\dfrac{1}{\sqrt{X^2 + E^2}}\right) - \dfrac{\pi A}{2}\end{array}\right]\right\}$$

The cask emitting radiation was represented as a cylinder with a 8.17 ft. diameter and a height of 13.0 ft. The casks receiving the thermal radiation of the emitting cask were represented as planes perpendicular to the line connecting the centerlines of the casks. View factors between casks with more than one intermediate cask between them are negligible.

Performing the integration and substituting the dimensional values,

$F_{Cask\text{-}Environment} = 0.62$.

The free convection coefficients are calculated based on the surface shape and position in Section 4.10.3. The above correlations are incorporated in ANSYS model via macros "HTOT_VPL.mac", "HTOT_HPD.mac", and "HTOT_HPU.mac". Air properties reported in Section 4.2 are used in these macros. The macros are provided in Section 4.12.

4.10.2 Total heat Transfer Coefficient to Ambient for Fire

The free convection heat transfer in Eq.4.10-1 is replaced with forced convection to analyze the fire accident case. A forced convection value of 4.5 Btu/hr-ft^2-°F (0.03125 Btu/hr-in^2-°F) is considered during the burning time from Reference [15].

The radiation heat transfer coefficient during burning period of the hypothetical fire accident, $h_{r,fire}$, is given by the following equation:

$$h_{r,fire} = \varepsilon_s F_{12}\left[\frac{\sigma\left(\varepsilon_f T_f{}^2 - T_s{}^2\right)}{T_f - T_s}\right] \quad \text{(Btu/hr-ft}^2\text{-°F)} \qquad \text{Eq. 4.10-4}$$

where,

ε_s= surface emissivity =0.8 [14]
ε_f = fire emissivity = 0.9 [14]
F_{12} = view factor from surface to fire = 1
$\sigma = 0.1714 \times 10^{-8}$ Btu/hr-ft^2-°R^4
T_f = surface temperature, 1475°F = 1935°R [14]
T_s = ambient temperature, °R

The calculated total heat transfer coefficients for the outer cask surfaces during the fire are listed in the Table 4.10-1 for various surface temperatures.

4.10.3 Free Convection Coefficients

The free convection coefficients are calculated based on the shape and position of the convective surface using correlations from Reference [4]. The convection correlations are described in the following sections.

4.10.3.1 Vertical Cylinder

Due to the large outer diameter of the cask, the convection coefficient on the cylindrical surface approaches that for a vertical flat plate. The following equations are used to calculate the free convection coefficients.

$$h_c = \frac{Nu\ k}{L}$$

with

L = height of the vertical plate
k = air conductivity

$$Nu = \left[(Nu_l)^m + (Nu_t)^m\right]^{1/m} \qquad with \quad m = 6 \quad for \ \ 1 < Ra < 10^{12}$$

$$Nu_l = \frac{2.8}{\ln(1 + 2.8/Nu^T)}$$ Nusselt number for fully laminar heat transfer with

$$Nu^T = \overline{C}_l\ Ra^{1/4} \quad , \ \overline{C}_l = 0.515 \ \text{(for gases)}$$

$$Nu_t = C_t^V\ Ra^{1/3}$$ Nusselt number for fully turbulent heat transfer with

$$C_t^V = \frac{0.13\,\mathrm{Pr}^{0.22}}{(1 + 0.61\,\mathrm{Pr}^{0.81})^{0.42}}$$

$$Ra = Gr\ \mathrm{Pr} \quad ; \quad Gr = \frac{g\,\beta\,(T_w - T_\infty)\,L^3}{\nu^2}$$

The correlations to calculate the total heat transfer coefficient are incorporated in the ANSYS model via “HTOT_VPL.mac”.

4.10.3.2 Horizontal Flat Surfaces Facing Downwards

$$h_c = \frac{Nu\ k}{L}$$

with

L = A/P
A=surface area of heated surface
P= perimeter of the heated surface
k = air conductivity

$$Nu = Nu_l \quad ; \qquad Nu_l = \frac{0.527\,Ra^{1/5}}{[1 + (1.9/\mathrm{Pr})^{9/10})^{2/9}}$$

$$Ra = Gr\ \mathrm{Pr} \quad ; \quad Gr = \frac{g\,\beta\,(T_w - T_\infty)\,L^3}{\nu^2}$$

The above correlations are incorporated in ANSYS model via macro ”HTOT_HPD.mac”

4.10.3.3 Horizontal Flat Plate Facing Upwards

$$h_c = \frac{Nu\ k}{L}$$

with

L = A/P
A=surface area of heated surface
P= perimeter of the heated surface
k = air conductivity

$$Nu = \left[(Nu_l)^m + (Nu_t)^m\right]^{1/m} \qquad with \quad m = 10 \quad for \quad Ra > 1$$

$$Nu_l = \frac{1.4}{\ln(1+1.4/Nu^T)}$$ Nusselt number for fully laminar heat transfer with

$$Nu^T = 0.835\,\overline{C}_l\,Ra^{1/4} \quad , \ \overline{C}_l = 0.515 \text{ (for gases)}$$

$$Nu_t = C_t^H\,Ra^{1/3}$$ Nusselt number for fully turbulent heat transfer

$C_t^H \approx 0.14$ for Pr < 100

$$Ra = Gr\ \mathrm{Pr} \quad ; \quad Gr = \frac{g\,\beta\,(T_w - T_\infty)\,L^3}{\nu^2}$$

The above correlations are incorporated in ANSYS model via macro ”HTOT_HPU.mac”.

4.11 Radial Hot Gap between the Basket Rails and the Cask Inner Shell

An average radial cold gap of 0.17" is considered between the basket and the cask cavity wall for the TN-68 cask, conforming to the gap specification, drawing 972-70-5 note 6. A radial, hot gap of 0.1" at thermal equilibrium is assumed in the ANSYS model for normal storage conditions. To verify this assumption, the radiuses of the inner shell and the basket can be calculated after thermal equilibrium using the following equation:

$$R_{hot} = R_{cold}\ (1 + \alpha\,(T_{avg} - 70))$$

α = mean coefficient of thermal expansion
T_{avg} = average component temperature

To calculate the hot radius of the basket, three locations are considered as shown in Figure 4.11-1. Locations I and II consist of stainless steel components of the basket and the aluminum component of the rails. Location III consists of basket and shim, which are stainless steel components only. Since adequate cold gaps are considered between the poison / aluminum plates and the stainless steel structural plates of the basket, the aluminum plates do not have any effect on the thermal growth of the basket.

The hot radius of the basket at locations I and II is calculated as follows:

$$R_{basket,hot,I} = R_{I,SS}\,(1 + \alpha_{SS}\,(T_{avg,SS} - 70)) + R_{I,Al}\,(1 + \alpha_{Al}\,(T_{avg,Al} - 70))$$

$$R_{basket,hot,II} = R_{II,SS}\,(1 + \alpha_{SS}\,(T_{avg,SS} - 70)) + R_{II,Al}\,(1 + \alpha_{Al}\,(T_{avg,Al} - 70))$$

The hot radius at location III is:

$$R_{basket,hot,III} = R_{III,SS}\,(1 + \alpha_{SS}\,(T_{avg,SS} - 70)) + L_{shim}\,(1 + \alpha_{SS}\,(T_{avg,shim} - 70))$$

The hot radius of the inner cask shell is:

$$R_{inner\ shell,hot} = R_{inner\ shell}\,(1 + \alpha_{shell}\,(T_{avg,shell} - 70))$$

The size of the radial hot gap is calculated as follows:
Hot gap = ($R_{inner\ shell,\ hot}$ - $R_{basket,\ hot}$)

The average temperatures are retrieved from result file of the base model basket at the hottest cross section ($71.18 \leq Z \leq 83.38$) for 100°F normal storage conditions using ANSYS [12] command "ETABLE". The ANSYS commands are collected in the file "AvgTempS.mac" in Section 4.12. The calculated hot dimensions are listed in Table 4.11-1.

The assumption of a 0.1" hot gap at thermal equilibrium is conservative, since the hot gaps shown in Table 4.11-1 are smaller than the assumed gap.

4.12 Supplemental Data

4.12.1 ANSYS Macros

This Section provides ANSYS macros utilized to calculate the heat transfer coefficients and the average component temperatures for the TN-68 cask thermal models. These macros are provided as part of a separate proprietary compact disc. A listing of the contents of the compact disc and a brief description of the macros are given below.

File Name	Description
HTOT_VPL.mac	Total heat transfer coefficient for vertical surfaces
HTOT_HPD.mac	Total heat transfer coefficient for horizontal, flat surfaces facing downwards
HTOT_HPU.mac	Total heat transfer coefficient for horizontal, flat surfaces facing upwards
AvgGasTemp.mac	Average gas temperature in the cask cavity
AvgTempS.mac	Average basket component temperatures for thermal / structural analyses

4.13 References

1. USNRC, SFPO, Interim Staff Guidance – 11, Rev. 3, "Cladding Considerations for the Transportation and Storage of Spend Fuel"
2. Environmental Conditions for On-Site Hazardous Material Packages, WHC-SD-TP-RPT-004, Westinghouse Hanford Company, 1992
3. Commonwealth Edison, "Typical BWR Average Axial Exposure Profiles", Memorandum NFS:BND:95-083, July 1995
4. Rohsenow, W. M., Hartnett, J. P., Ganic, E. N. , "Handbook of Heat Transfer Fundamentals", 2nd Edition, 1985
5. ASME Boiler and Pressure Vessel Code, Section II, Part D, "Material Properties", 1998 and 2000 addenda
6. Perry, R. H., Chilton, C. H., "Chemical Engineers' Handbook", 5th Edition, 1973
7. Zoldners, N. G., "Thermal Properties of Concrete under Sustained Elevated Temperatures", ACI Publications, Paper SP 25-1, American Concrete Institute, Detroit, MI, 1970
8. Bentz, D. P., "A Computer Model to Predict the Surface Temperature and Time-of-wetness of Concrete Pavements and Bridge Decks", Report # NISTIR 6551, National Institute of Standards and Technology, 2000
9. Siegel, Robert, Howell, R. H., "Thermal Radiation Heat Transfer", 4th Edition, 2002
10. Azzazy Technology Inc., "Emissivity Measurements of 304 Stainless Steel", Report Number ATI-2000-09-601, 2000
11. USNRC, SFPO, NUREG-1536, "Standard Review Plan for Dry Cask Storage Systems - Final Report", 1997
12. ANSYS Computer Code and User's Manuals, Version 6.0 and 8.0.
13. Viebrock, J. M., Douglas, H. M., "Domestic Light Water Reactor Fuel Design Evolution", Vol. III, Nuclear Assurance Corporation, 1981
14. USNRC, Code of Federal Regulations, Part 71, "Packaging and Transportation of Radioactive Material", 2004
15. Gregory, J. J., Mata, R., Keltner, N. R., "Thermal Measurements in a Series of Long Pool Fires", SANDIA Report, SAND 85-0196, TTC-0659,1987
16. IAEA Safety Standards, "Regulations for the Safe Transport of Radioactive Material", 1985
17. USNRC, SFPO, NUREG/CR-0497, "A Handbook of Materials Properties for Use in the Analysis of Light Water Reactor Fuel Rod Behavior", MATPRO - Version II (Revison 2), EG&G Idaho, Inc., TREE-1280, 1981
18. Oak Ridge National Laboratory, RSIC Computer Code Collection, "SCALE, A Modular Code System for Performing Standardized Computer Analysis for Licensing Evaluation for Workstations and Personal Computers", NUREG/CR-0200, Rev. 6, ORNL/NUREG/CSD-2/V3/R6
19. SANDIA Report, SAND90-2406, "A Method for Determining the Spent Fuel Contribution to Transport Cask Containment Requirements", 1992
20. Transnuclear, Inc., "Safety Analysis Report, NUHOMS®-MP197 Multipurpose Cask – Transportation Package", Rev. 0, Appendix 3.7.1

Table 4.3-1
Maximum Temperatures for Normal Storage Conditions, 100°F Ambient

	Maximum Temperature (°F)			
Component	**Design Basis Model**	**Basket Alternate I**	**Basket Alternate II**	**Temp Limit (°F)**
Fuel Cladding	622	612	617	752 [1]
Basket	595	586	591	
Basket Rails, type 1&2	382	382	382	
Basket Shim	350	349	351	
Inner Shell	319	319	319	
Gamma Shield	314	314	314	
Radial Neutron Shield	295	295	295	300
Top Neutron Shield	211	211	211	220
Cask Outer Surface	255	255	255	
Cask Lid Seal	212	211	211	536
Vent & Port Seals	212	211	211	536
Average Temp at Hottest Cross Section				
Basket	479			
Basket Rails, type 1&2	366			
Inner Shell	316			
Aluminum Plate, A	513			
Stainless Steel Bar, A	513			

Table 4.3-2
Maximum Temperatures for Normal Storage Conditions, -20°F Ambient

	Maximum Temperature (°F)
Component	**Design Basis Model**
Fuel Cladding	533
Basket	502
Basket Rails, type 1&2	281
Basket Shim	247
Inner Shell	213
Gamma Shield	208
Radial Neutron Shield	188
Top Neutron Shield	103
Cask Outer Surface	148
Cask Lid Seal	103
Vent & Port Seals	103
Average Temp at Hottest Cross Section	
Basket	382
Basket Rails, type 1&2	265
Inner Shell	211
Aluminum Plate, A	418
Stainless Steel Bar, A	418

Table 4.4-1
Maximum Temperatures for Hypothetical Fire Accident

Component	Temperature (°F)	Time (hr)	Solution Type	Allowable Limit (°F)
Fuel Cladding	737	∞	Steady State	1058 [1]
Basket	717	∞	Steady State	
Outer Shell	842	0.25	Transient	
Lid Seal	470	0.27	Transient	536
Vent & Port Seals	411	0.27	Transient	536

Table 4.4-2
Maximum Temperatures for Postulated Buried Cask Accident

Component	Temperature (°F)	Time (hr)	Solution Type	Allowable Limit (°F)
Fuel Cladding	1058	90	Transient	1058 [1]
Radial Neutron Shield	300	0.6	Transient	300*
Top Neutron Shield	300	38	Transient	300
Lid Seal†	503	120	Transient	536
Vent & Port Seals	490	120	Transient	536

* 300°F is the long-term temperature limit for radial neutron shield material
† The analysis is run only for 120 hr after the buried cask accident case occurs

Table 4.5-1
Average Heat up Rates

Average Heat up Rate of TN68 Cask with water in the cavity

Component	Material	Volume (in^3)	Weight (lbm)	Cp (Btu/lbm-°F)	Cp × M Btu/°F
Fuel Assembly	---	158267	47940	0.0576	2761
Fuel Compartment	SA240, type 304	51752	15008	0.114	1711
Structural Plates	SA240, type 304	8162	2367	0.114	270
Basket Shim	SA240, type 304	3607	1046	0.114	119
Basket Plates	Aluminum 1100	44071	4319	0.216	933
Rails Type 1 & 2	Aluminum 6061	27194	2665	0.215	573
Cask Inner Shell	SA203, Gr. E	331105	94365	0.105	9908
Cask Bottom	SA516, Gr. 70	54677	15583	0.105	1636
Cask Outer Shell	SA516, Gr. 70	39221	11178	0.105	1174
Neutron Shield Boxes	Aluminum 6063	25531	2502	0.215	538
Solid Neutron Shield	Polymer	244860	13957	0.311	4341
Water in Cavity	---	365574	13234	1.0	13234
Total		1354021	224164		37193

Average heat up rate = $\frac{102369}{37193} = 2.8$ °F/hr

Average Heat up Rate of TN68 Cask without water in the cavity

Component	Material	Volume (in^3)	Weight (lbm)	Cp (Btu/lbm-°F)	Cp × M Btu/°F
Fuel Assembly	---	158267	47940	0.0576	2761
Fuel Compartment	SA240, type 304	51752	15008	0.114	1711
Structural Plates	SA240, type 304	8162	2367	0.114	270
Basket Shim	SA240, type 304	3607	1046	0.114	119
Basket Plates	Aluminum 1100	44071	4319	0.216	933
Rails Type 1 & 2	Aluminum 6061	27194	2665	0.215	573
Cask Inner Shell	SA203, Gr. E	331105	94365	0.105	9908
Cask Bottom	SA516, Gr. 70	54677	15583	0.105	1636
Cask Outer Shell	SA516, Gr. 70	39221	11178	0.105	1174
Neutron Shield Boxes	Aluminum 6063	25531	2502	0.215	538
Solid Neutron Shield	Polymer	244860	13957	0.311	4341
Water in Cavity	---	0	0	1.0	0
Total		988447	210930		23967

Average heat up rate = $\frac{102369}{23967} = 4.3$ °F/hr

Table 4.5-2
Temperatures for the Vacuum Drying Process Without Helium Backfill

Component	**30kW Heat Load Transient Run Max Temp (°F)**	**25.25kW Heat Load Steady Sate Run Max Temp (°F)**	**Allowable Limit (°F)**
Fuel Cladding	752 @ 37 hr	749	752 [1]
Radial Neutron Shield	225 @ 37 hr	251	300

Average temperatures at hottest section for thermal expansion analysis

	Vacuum 30kW @ 30 hrs 0.1" hot gap	Vacuum 30kW @ 30 hrs 0.0 hot gap
Basket	534	433
Aluminum Rail	400	258
Cask Inner Shell	223	252
Aluminum Plate, A	568	479
Aluminum Plate, B	563	466
Aluminum Plate, C	434	304
Aluminum Plate, D	364	264
Stainless Steel Bar, A	567	477
Stainless Steel Bar, B	562	465
Stainless Steel Bar, C	435	306
Stainless Steel Bar, D	367	266

Table 4.5-3
Temperatures for Vacuum Drying with Helium Backfill at 30 Hours

Component	**30kW Heat Load Transient Run Vacuum Max Temp (°F)**	**30kW Heat Load Steady State Run Helium Max Temp (°F)**	**Allowable Limit (°F)**
Fuel Cladding	711 @ 30 hrs[*]	596	752 [1]
Radial Neutron Shield	[†]	230	300

[*] See Figure 4.5-1b
[†] Maximum temperature is achieved in steady state conditions, see Figure 4.5-1b

Table 4.6-1
Minimum Height of Fuel Rubble*

GE designation	GE2	GE4	GE5, GE8, type I	GE8, type II
TN ID	7x7 – 49/0	8x8 – 63/1	8x8 – 62/2	8x8 – 60/4
Cladding area (in^2)	2.62	3.14	2.92	2.87
Cladding volume (in^3)	377	458	438	430
Pellet area (in^2)	9.13	8.56	8.19	7.92
UO2 volume (in^3)	1314	1250	1228	1188
H_{min} (in)	57	57	56	54

GE designation	GE9, GE10	GE11, GE13	GE12
TN ID	8x8 – 60/1	9x9 – 74/2	10x10 – 92/2
Cladding area (in^2)	2.88	2.86	3.02
Cladding volume (in^3)	433	418	453
Pellet area (in^2)	7.96	8.22	8.60
UO2 volume (in^3)	1194	1200	1290
H_{min} (in)	54	54	58

* See Table 5.2-1 for fuel characteristics and Section 4.8.2 for fuel material properties

Table 4.6-2
Maximum Temperature for the Cask with 8 Damaged Fuel Assemblies, Normal Storage Conditions

Component	Maximum Temperature (°F)	Temp. Limit (°F)
Intact Fuel cladding	622	752 [1]
Basket	596	
Basket Rails, type 1&2	383	
Basket Shim	349	
Cask Inner Shell	319	
Gamma Shield	314	
Radial Neutron Shield	295	300
Top Neutron Shield	211	220
Cask Outer Surface	255	
Cask Lid Seal	212	536
Vent & Port Seals	211	536

Table 4.6-3
Maximum Temperature for the Cask with 8 Damaged Fuel Assemblies, Accident Conditions

Component	Maximum Temperature (°F)	Temp. Limit (°F)
Fuel Cladding	636	1058 [1]
Basket	610	
Cask Outer Shell	274	
Lid Seal	227	536
Vent & Port Seals	226	536

Table 4.8-1
Effective Properties for Intact Fuel Assembly

T_s (°F)	T_o (°F)	T_{avg} (°F)	$k_{eff,tr}$ in Helium (Btu/hr-in-°F)
100	155	**128**	**1.396E-02**
200	248	**224**	**1.622E-02**
300	341	**321**	**1.880E-02**
400	436	**418**	**2.172E-02**
500	531	**515**	**2.514E-02**
600	627	**613**	**2.900E-02**
700	723	**712**	**3.312E-02**
800	821	**810**	**3.768E-02**
900	918	**909**	**4.272E-02**
1000	1016	**1008**	**4.829E-02**
1100	1114	**1107**	**5.518E-02**
Q_{react} (Btu/hr-in)	10.487		

T_s (°F)	T_o (°F)	T_{avg} (°F)	$k_{eff,tr}$ in Vacuum (Btu/hr-in-°F)
100	256	**178**	**4.938E-03**
200	325	**263**	**6.163E-03**
300	401	**350**	**7.684E-03**
400	481	**440**	**9.547E-03**
500	566	**533**	**1.179E-02**
600	653	**627**	**1.445E-02**
700	744	**722**	**1.756E-02**
800	837	**818**	**2.114E-02**
900	931	**915**	**2.523E-02**
1000	1026	**1013**	**2.971E-02**
1100	1122	**1111**	**3.512E-02**
Q_{react} (Btu/hr-in)	10.487		

Assembly Type	GE4	GE5, GE8-Type I	GE8-Type II	GE9, GE10	GE11, GE13	GE 12
A_{zirc}, (in^2)	3.089	2.812	2.722	2.722	2.683	2.842
$k_{eff,axl}$ (Btu/hr-in-°F)	0.0516	0.0470	0.0455	0.0455	**0.0449**	0.0475
V_{UO2} (in^3)	1,233.05	1,178.72	1,140.70	1,146.27	1,183.20	1,238.45
V_{zirc} (in^3)	444.83	404.90	391.93	391.90	386.37	409.22
ρ_{eff} (lbm/in^3)	0.115	0.109	**0.105**	0.106	0.108	0.113
M_{UO2}, lbm	488.3	466.8	451.7	453.9	468.5	490.4
M_{zirc}, lbm	105.4	96.0	92.9	92.9	91.6	97.0
M_{tot}, lbm	593.7	562.8	544.6	546.8	560.1	587.4
$C_{p,fuel}$ (Btu/lbm-°F)	0.0577	0.0577	0.0577	**0.0576**	0.0576	0.0576

Table 4.8-2
Effective Conductivity for Damaged Fuel Assembly

Temperature	Transverse Effective Conductivity [20]
(°F)	(Btu/hr-in-°F)
120	0.0113
217	0.0133
315	0.0156
413	0.0182
511	0.0212
609	0.0246
Axial Effective Conductivity = 0.0449* × 0.9 = 0.0404 Btu/hr-in-°F	

* 0.0449 Btu/hr-in-°F is the minimum axial effective conductivity calculated for the intact fuel assemblies

Table 4.9-1
Average Peaking Factors

	Height from Bottom of Active Fuel (in)	P_i (measured)	P_i (interpolated)	A_i	$P_{avg, i}$
1	0.00	0.000			
	2.17		0.151	0.164	0.075
2	2.88	0.200			
	8.2		0.671	2.441	0.405
3	8.64	0.710			
	11.69		0.837	2.663	0.763
4	12.24	0.860			
	14.37		0.959	2.404	0.897
5	14.40	0.960			
	20.40		1.080	6.150	1.020
6	20.88	1.090			
	23.89		1.116	3.841	1.101
7	24.34	1.120			
	26.57		1.136	3.018	1.126
8	27.22	1.140			
	30.84		1.168	4.917	1.152
9	32.40	1.180			
	36.09		1.180	6.186	1.178
10	36.72	1.180			
	43.04		1.198	8.256	1.188
11	43.92	1.200			
	60.49		1.200	20.939	1.200
12	60.91	1.200			
	77.44		1.200	20.340	1.200
13	77.76	1.200			
	81.40		1.194	4.740	1.197
14	83.52	1.190			
	84.89		1.182	4.152	1.190
15	85.25	1.180			
	87.57		1.174	3.156	1.178
16	89.28	1.170			
	93.60		1.153	7.022	1.164
17	94.32	1.150			
	97.09		1.141	4.002	1.147
18	97.344	1.140			
	99.77		1.131	3.045	1.136
19	100.08	1.130			
	105.79		1.090	6.690	1.111

Table 4.9-1
Average Peaking Factors – Continued

	Height from Bottom of Active Fuel (in)	**P_i (measured)**	**P_i (interpolated)**		**$P_{avg, i}$**
20	107.28	1.080			
	107.61		1.079	1.973	1.084
21	109.58	1.070			
	111.97		1.063	4.665	1.070
22	113.04	1.060			
	116.24		1.016	4.457	1.044
23	117.36	1.000			
	119.75		0.956	3.466	0.987
24	121.68	0.920			
25	123.12	0.900			
	124.02		0.879	3.921	0.918
26	129.60	0.750			
	133.69		0.615	7.337	0.759
27	135.36	0.560			
	140.64		0.230	3.067	0.441
28	141.12	0.200			
	144.00		0.000	0.391	0.116
29	144.00	0.000			

Table 4.9-2
Peaking Factors Applied in Finite Element Model

Region #	Height (in)		Z-axis in FEM		Peaking Factor
	from	to	from	to	
1	0.00	2.17	8.01	10.18	0.075
2	2.17	8.20	10.18	16.21	0.405
3	8.20	11.69	16.21	19.70	0.763
4	11.69	14.37	19.70	22.38	0.897
5	14.37	20.40	22.38	28.41	1.020
6	20.40	23.89	28.41	31.90	1.101
7	23.89	26.57	31.90	34.58	1.126
8	26.57	30.84	34.58	38.85	1.152
9	30.84	36.09	38.85	44.10	1.178
10	36.09	43.04	44.10	51.05	1.188
11	43.04	60.49	51.05	68.50	1.200
12	60.49	77.44	68.50	85.45	1.200
13	77.44	81.40	85.45	89.41	1.197
14	81.40	84.89	89.41	92.90	1.190
15	84.89	87.57	92.90	95.58	1.178
16	87.57	93.60	95.58	101.61	1.164
17	93.60	97.09	101.61	105.10	1.147
18	97.09	99.77	105.10	107.78	1.136
19	99.77	105.79	107.78	113.80	1.111
20	105.79	107.61	113.80	115.62	1.084
21	107.61	111.97	115.62	119.98	1.070
22	111.97	116.24	119.98	124.25	1.044
23	116.24	119.75	124.25	127.76	0.987
24	119.75	124.02	127.76	132.03	0.918
25	124.02	133.69	132.03	141.70	0.759
26	133.69	140.64	141.70	148.65	0.441
27	140.64	144.00	148.65	152.01	0.116

Table 4.10-1
Total Heat Transfer Coefficient during Fire

T_s	h_{forced} *	h_r †	H_{tot}
(°F)	(Btu/hr-in^2-°F)	(Btu/hr-in^2-°F)	(Btu/hr-in^2-°F)
251	0.03125	0.0962	0.1274
301	0.03125	0.0996	0.1309
351	0.03125	0.1032	0.1345
401	0.03125	0.1070	0.1382
451	0.03125	0.1109	0.1422
501	0.03125	0.1150	0.1463
551	0.03125	0.1193	0.1505
601	0.03125	0.1237	0.1549
651	0.03125	0.1282	0.1595
701	0.03125	0.1329	0.1641
751	0.03125	0.1377	0.1689
801	0.03125	0.1425	0.1738
851	0.03125	0.1475	0.1787
901	0.03125	0.1524	0.1836
951	0.03125	0.1573	0.1885
1001	0.03125	0.1619	0.1932
1051	0.03125	0.1663	0.1975
1101	0.03125	0.1701	0.2013
1151	0.03125	0.1729	0.2041
1201	0.03125	0.1740	0.2052
1251	0.03125	0.1720	0.2033

* 0.03125 Btu/hr-in^2-°F = 4.5 Btu/hr-ft^2-°F

† The radiation heat transfer coefficient, h_r, is given by the equation:

$$h_r = \varepsilon_s F_{sf} \left[\frac{\sigma \left(\varepsilon_f T_f^{\,2} - T_s^{\,2} \right)}{T_f - T_s} \right] \qquad \text{(Btu/hr-in}^2\text{-°F)}$$

where ε_s = surface emissivity = 0.8 [14]
ε_f = fire emissivity = 0.9 [14]
F_{sf} = view factor from surface to fire =1
$\sigma = 0.119 \times 10^{-10}$ Btu/hr-in^2-°R^4
T_s = surface temperature, °R
T_f = fire temperature =1475°F = 1935°R [14]

Table 4.11-1
Hot Gap between the Basket and the Cask Inner Shell

ID Cask =69.5" Hottest Cross Section	Cold Dimension	T_{avg} (Table 4.3-1)	Material	α *	Hot Dimension
	(in)	(°F)	(---)	(in/in-°F)	(in)
$R_{SS,I}$	27.75	479	SA240, type 304	9.66E-06	27.860
$R_{Al,I}$	6.83	366	Al-6061	1.35E-05	6.857
$R_{basket,I}$	34.58				34.717
$R_{inner\ shell}$	34.75	316	SA203, Grade E	6.93E-06	34.809
Radial gap I	0.17				0.092
$R_{SS,II}$	28.58	479	SA240, type 304	9.66E-06	28.693
$R_{Al,II}$	6.00	366	Al-6061	1.35E-05	6.024
$R_{basket,II}$	34.58				34.717
$R_{inner\ shell}$	34.75	316	SA203, Grade E	6.93E-06	34.809
Radial gap II	0.17				0.092
$R_{SS,III}$	33.78	479	SA240, type 304	9.66E-06	33.913
$L_{Shim,III}$	0.8	344	SA240, type 305	9.29E-06	0.802
$R_{basket,III}$	34.58				34.715
$R_{inner\ shell}$	34.75	316	SA203, Grade E	6.93E-06	34.809
Radial gap III	0.17				0.094

ID Cask =69.75" Hottest Cross Section	Cold Dimension	T_{avg} (Table 4.3-1)	Material	α *	Hot Dimension
	(in)	(°F)	(---)	(in/in-°F)	(in)
$R_{SS,I}$	27.75	479	SA240, type 304	9.66E-06	27.860
$R_{Al,I}$	6.955	366	Al-6061	1.35E-05	6.983
$R_{basket,I}$	34.705				34.842
$R_{inner\ shell}$	34.875	316	SA203, Grade E	6.93E-06	34.934
Radial gap I	0.17				0.092
$R_{SS,II}$	28.58	479	SA240, type 304	9.66E-06	28.693
$R_{Al,II}$	6.13	366	Al-6061	1.35E-05	6.149
$R_{basket,II}$	34.705				34.842
$R_{inner\ shell}$	34.875	316	SA203, Grade E	6.93E-06	34.934
Radial gap II	0.17				0.092
$R_{SS,III}$	33.905	479	SA240, type 304	9.66E-06	34.039
$L_{Shim,III}$	0.8	344	SA240, type 305	9.29E-06	0.802
$R_{basket,III}$	34.705				34.841
$R_{inner\ shell}$	34.875	316	SA203, Grade E	6.93E-06	34.934
Radial gap III	0.17				0.094

* Interpolated from values in Reference [4.1]

Figure 4.3-1
Finite Element Model of TN-68 Cask

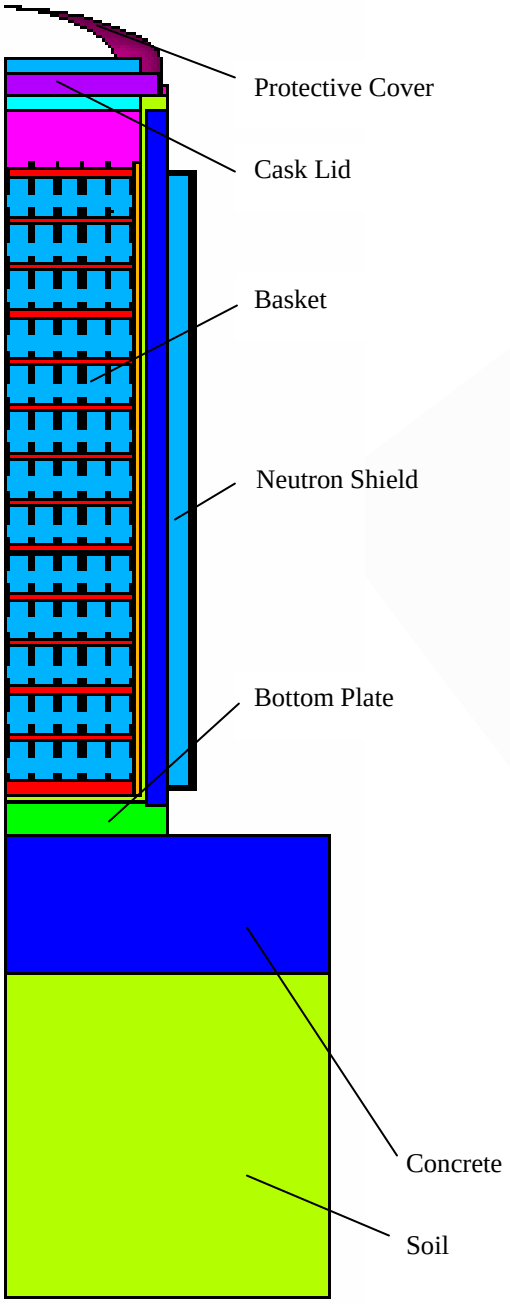

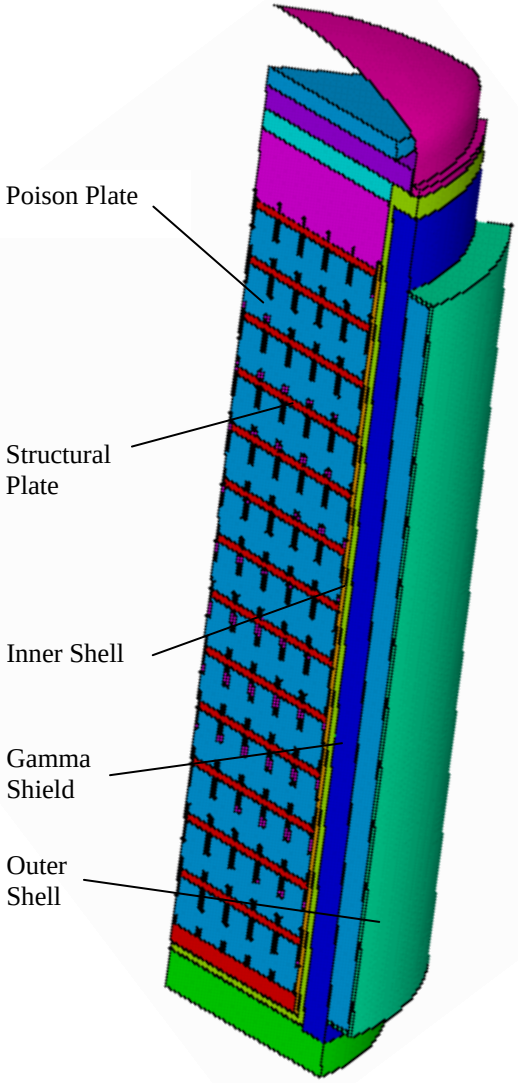

Figure 4.3-2
Details of the FEM, TN-68 Cask – Design Basis Basket

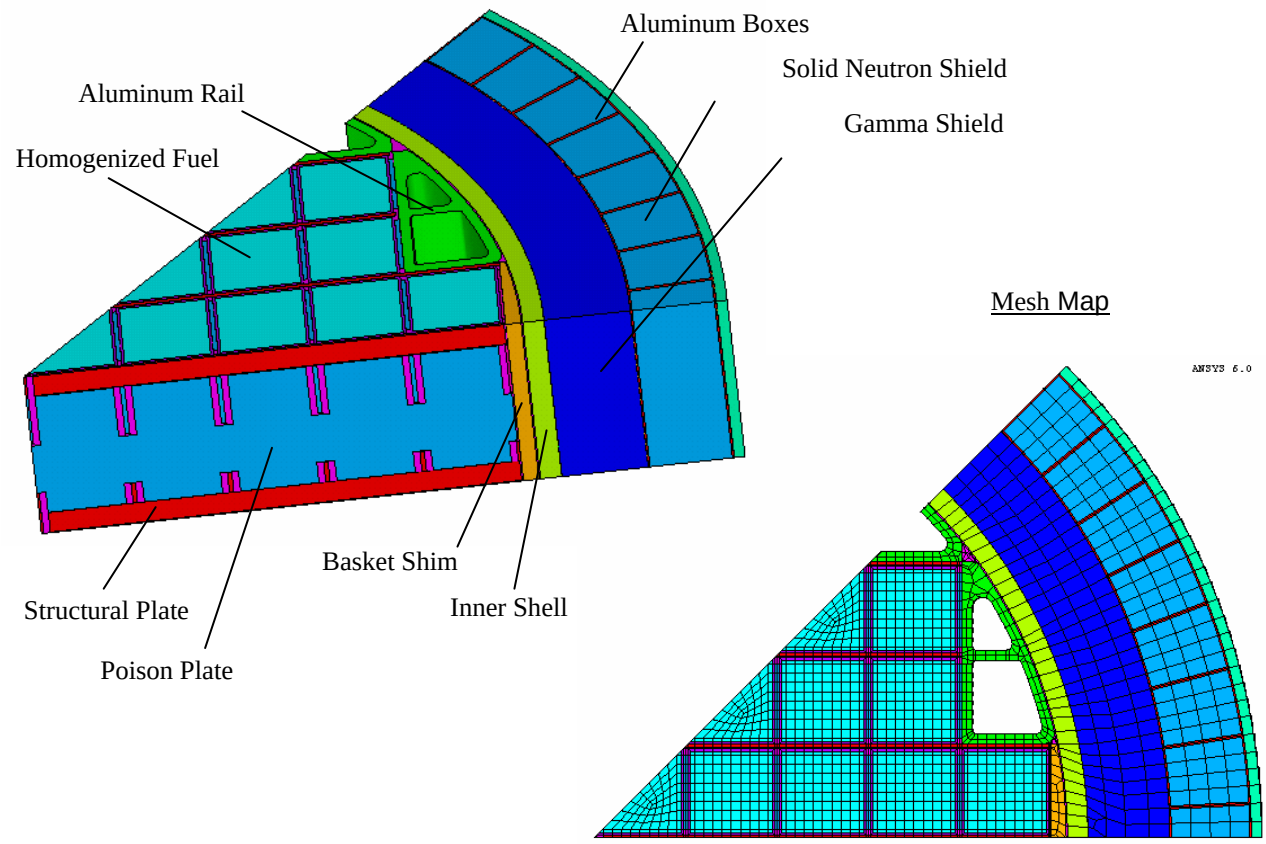

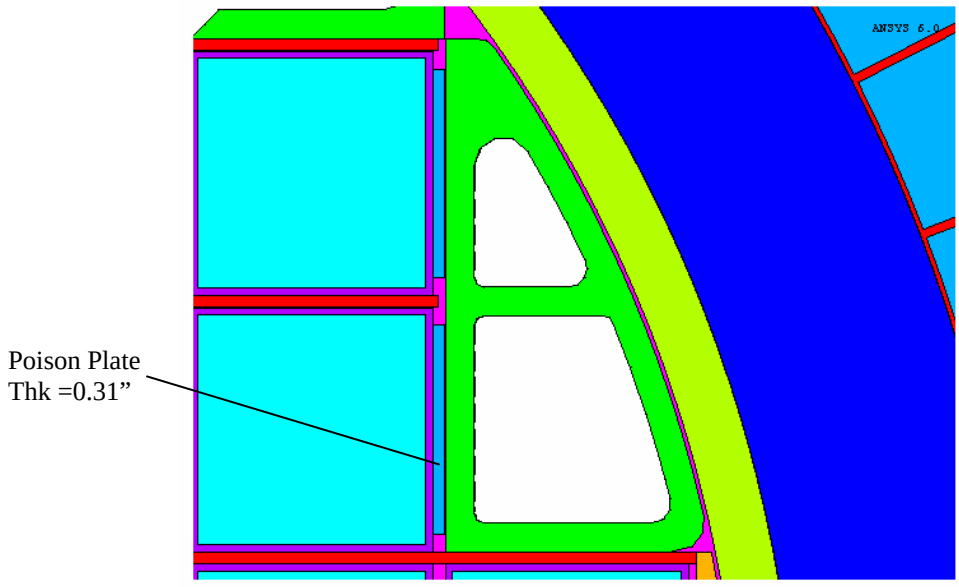

Figure 4.3-3
Details of the FEM, TN-68 Cask – Alternate Basket Details

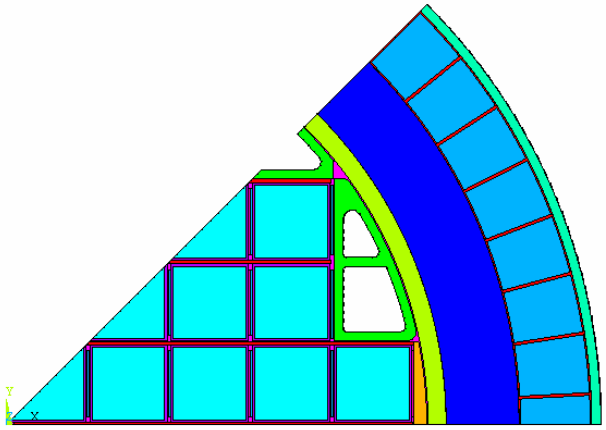

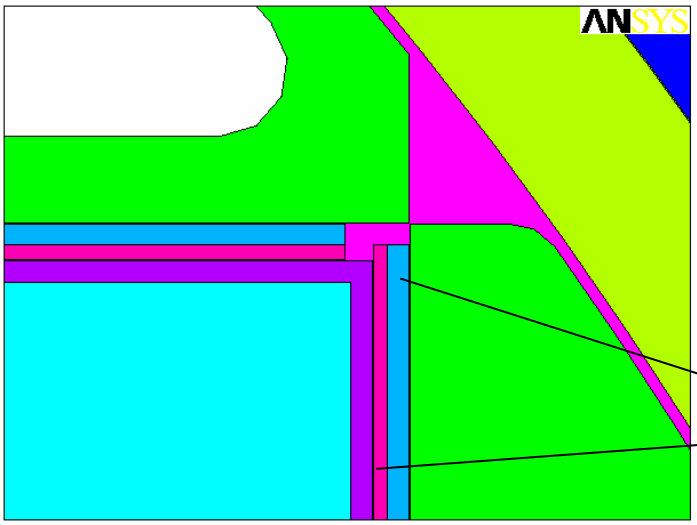

Basket Alternate I

Poison Plate, Thk = 0.1875”

Aluminum Plate, Thk = 0.1225”

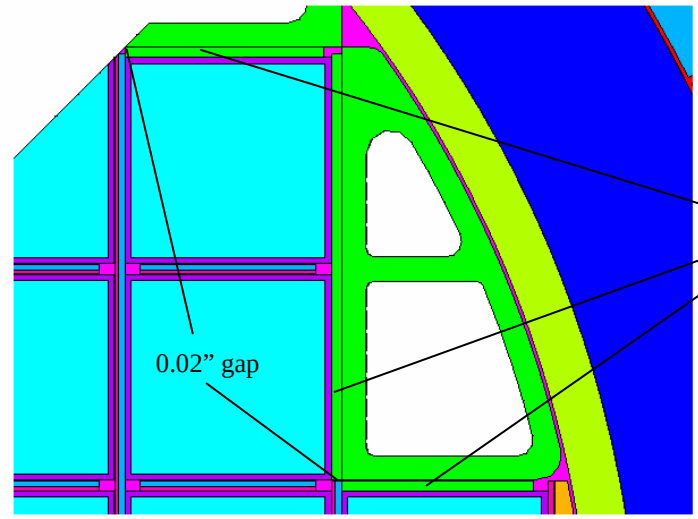

Basket Alternate II

Paired aluminum /poison plates at these locations are replaced by Al-6061 plates

Figure 4.3-4
Typical Boundary Conditions

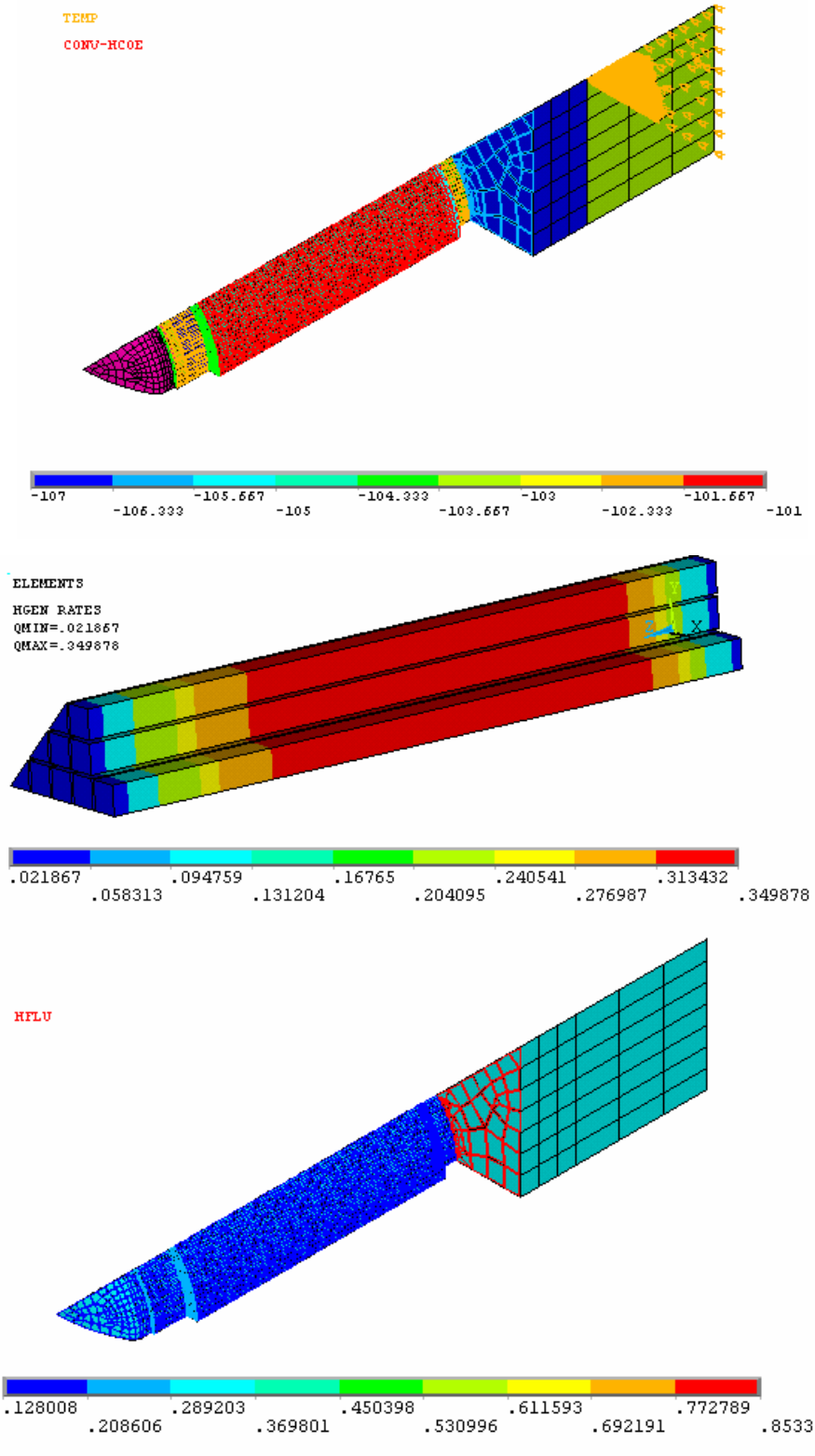

Figure 4.3-5
Temperature Distribution in TN68 Cask – Design Basis Model

Entire Cask Model

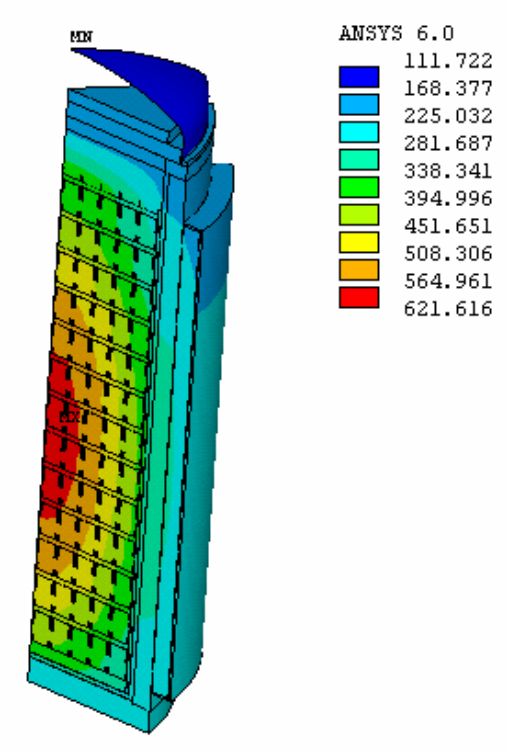

Homogenized Fuel Assemblies

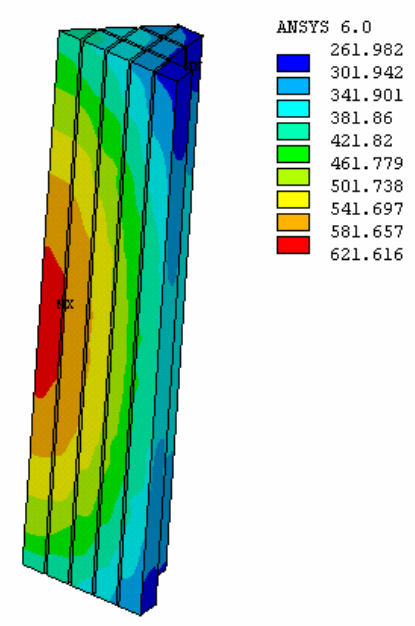

Basket Rails

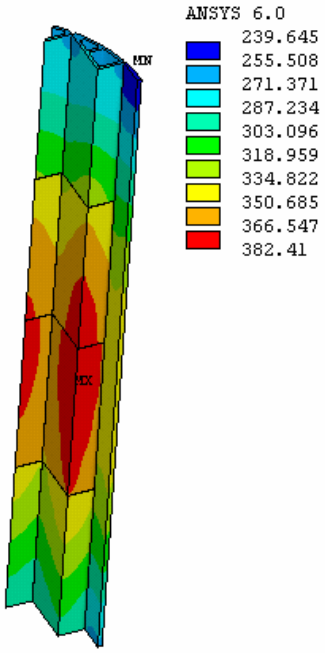

Basket

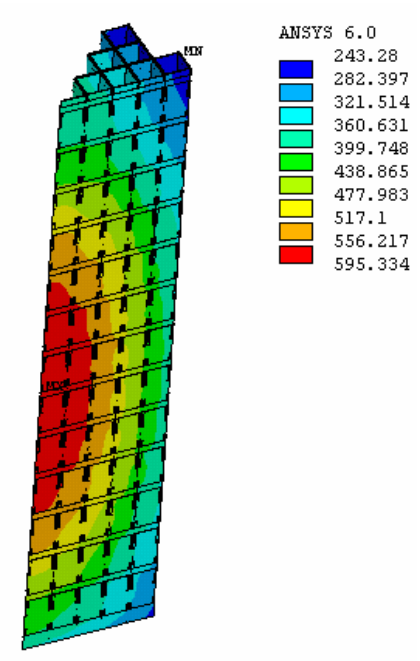

Solid Neutron Shield

Cask Body

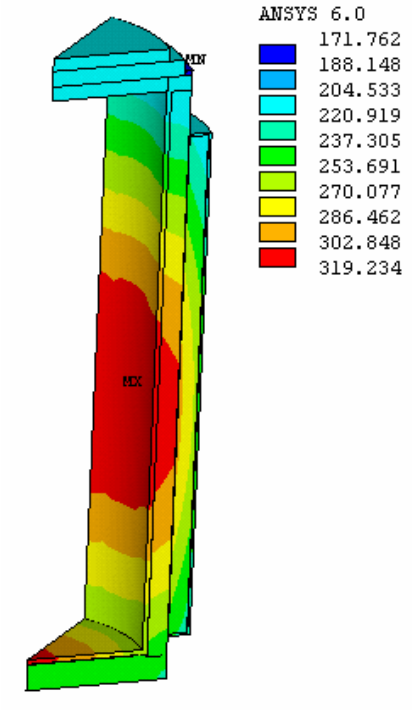

Figure 4.3-6
Temperature Distribution in TN68 Cask – Alternates

TN-68 Cask Alternate I

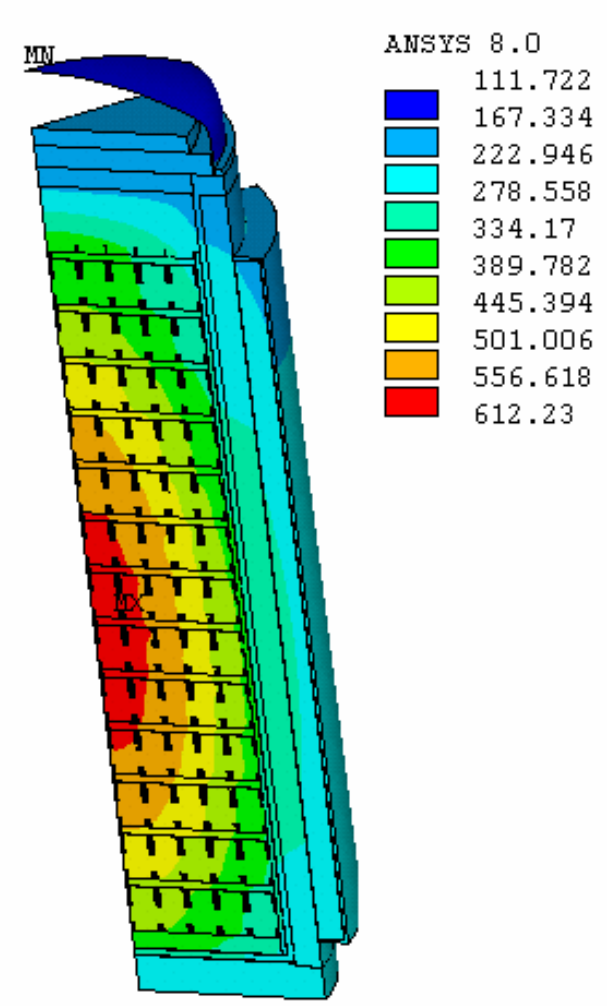

TN-68 Cask Alternate II

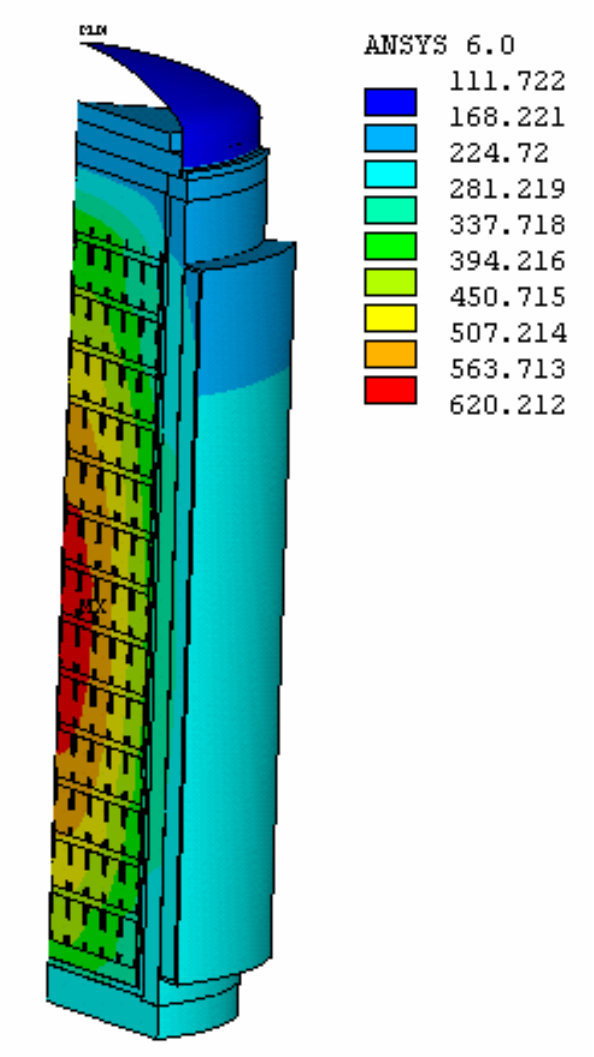

Figure 4.4-1
Cross-Section and Lid-Seal Models

Cross-Section Model

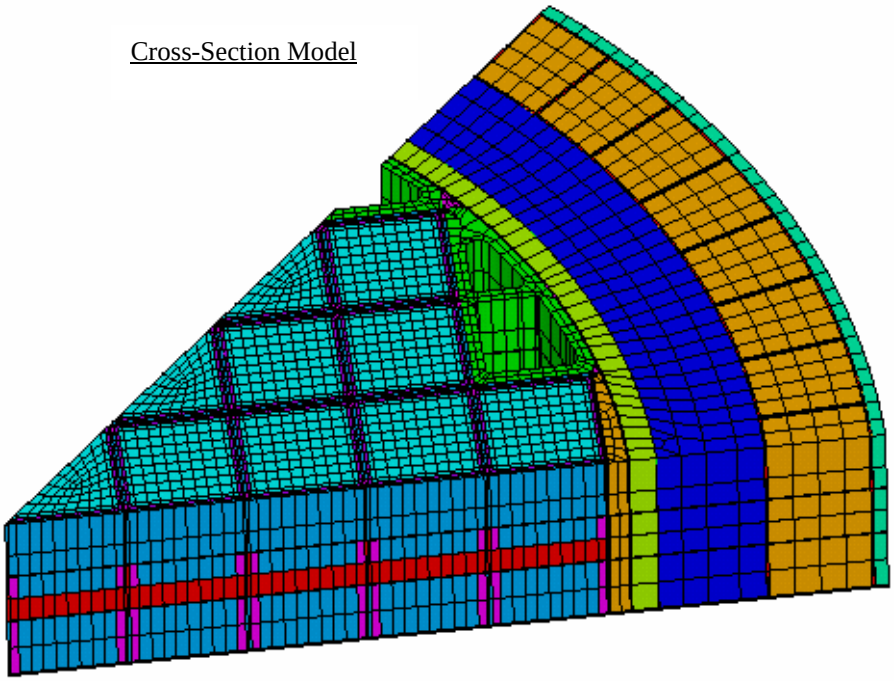

Lid-Seal Model

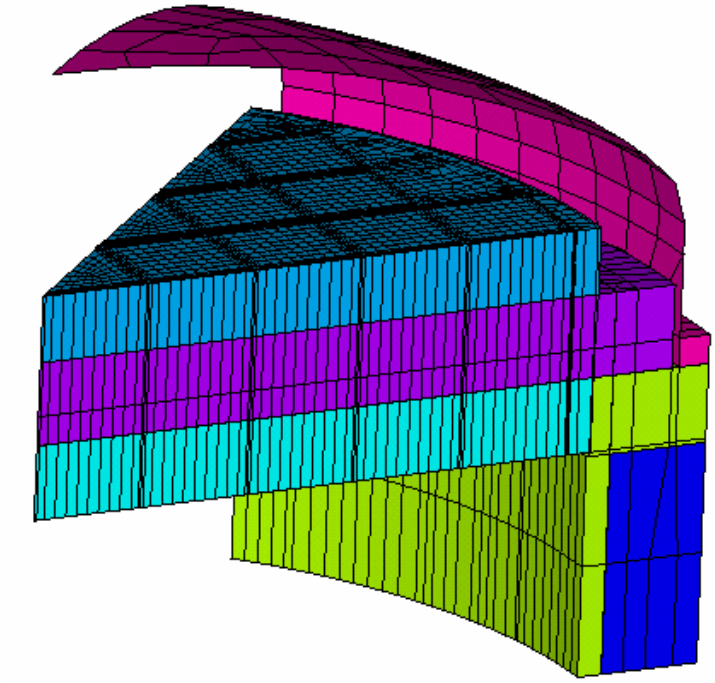

Figure 4.4-2
Location of Heat Fluxes on Lid-Seal Model

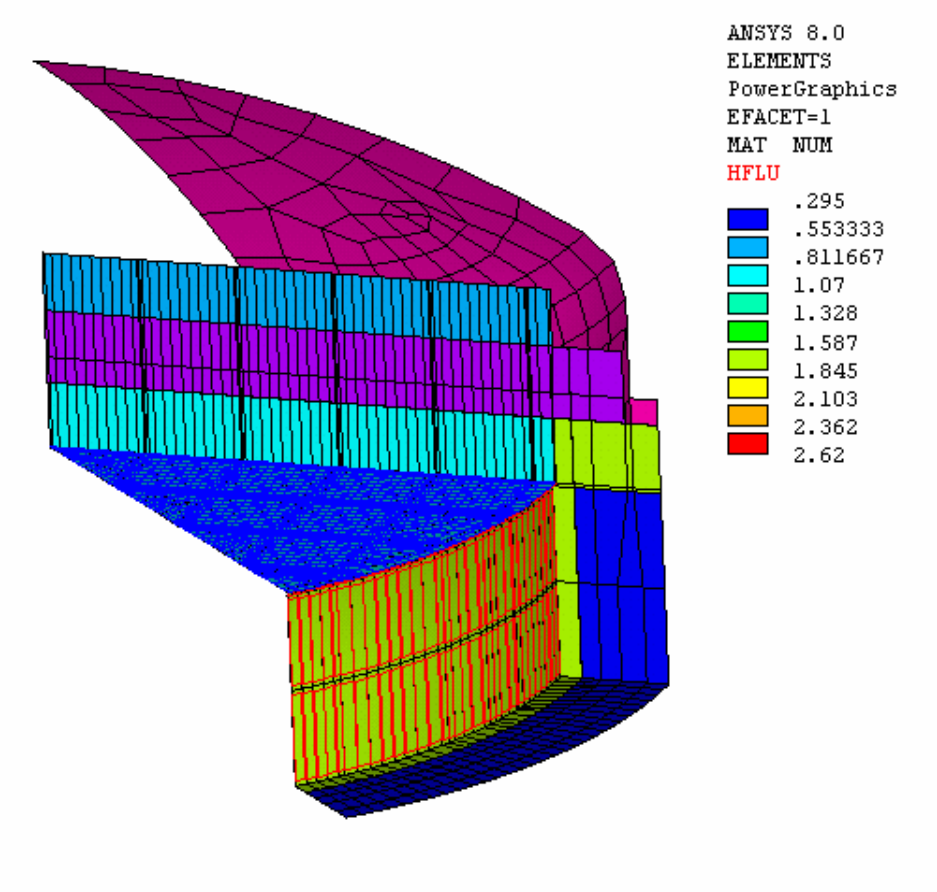

Figure 4.4-3
Time-Temperature Histories for Hypothetical Fire Accident

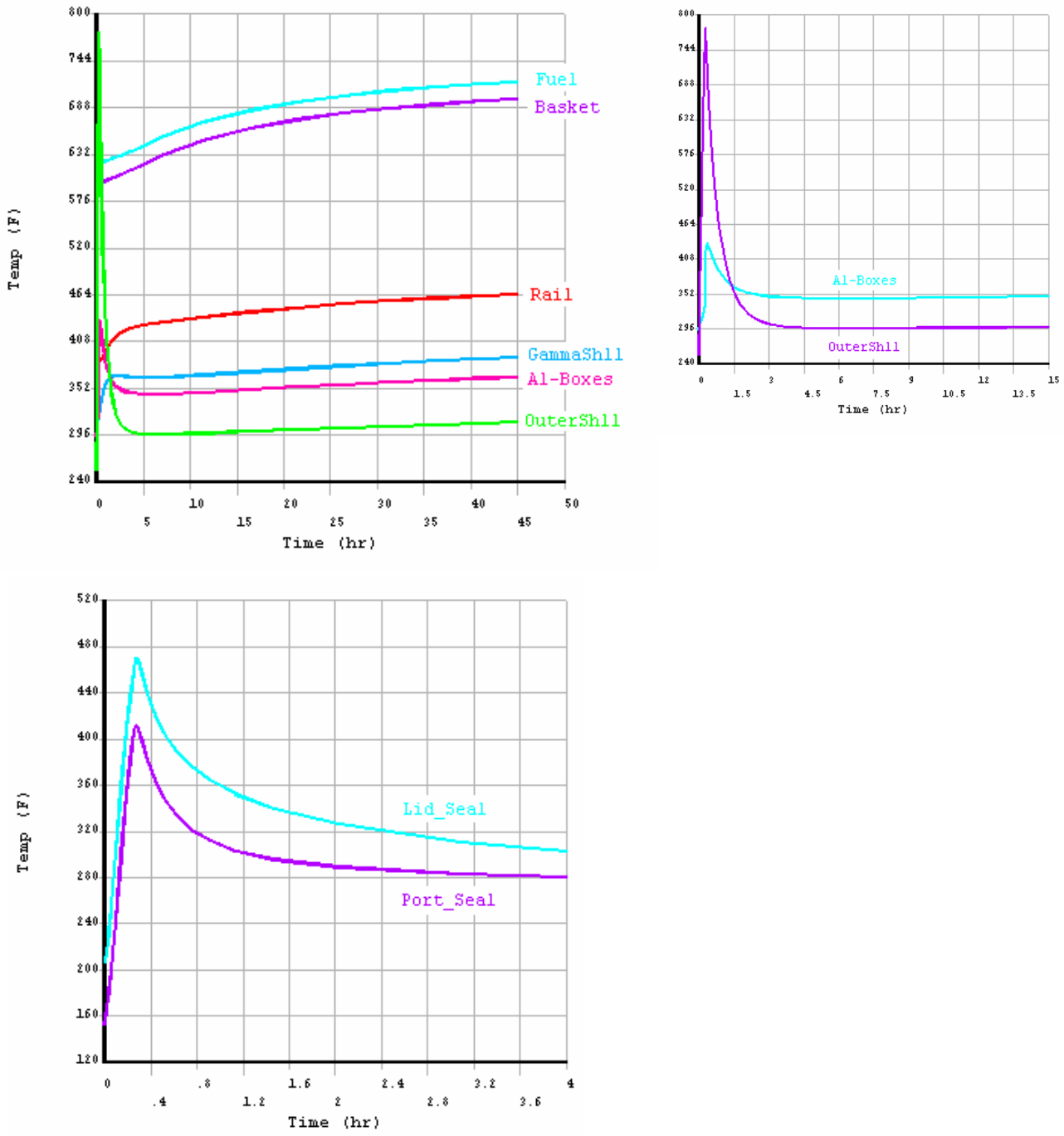

Figure 4.4-4
Temperature Distributions for Hypothetical Fire Accident

Steady State Run of Cross-Section Model

Entire Model

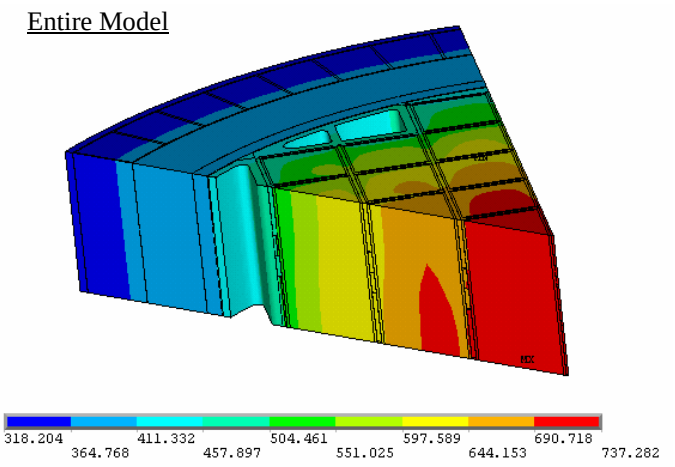

Fuel Assemblies

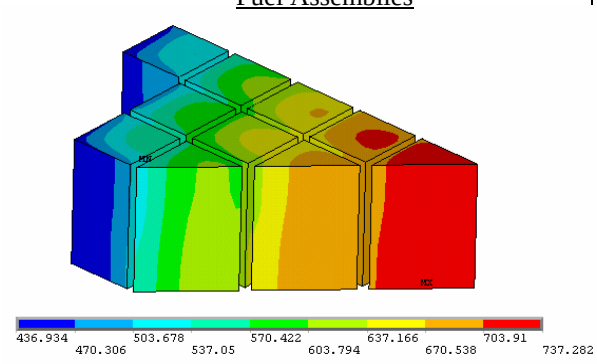

Basket and Rails

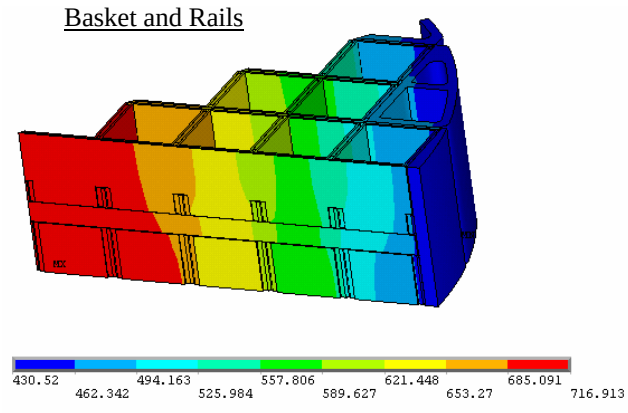

Cask Body

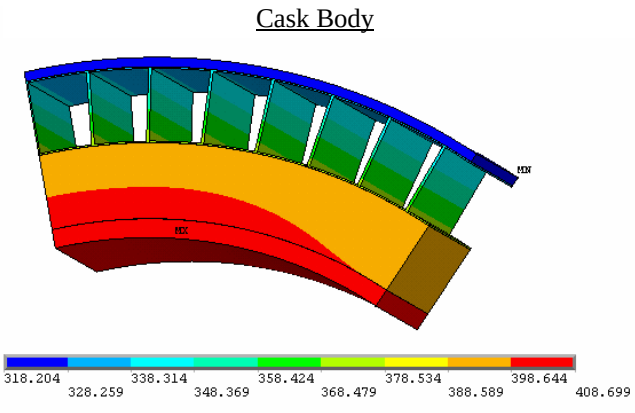

Transient Run of Lid-Seal Model – 36 Hours after Fire Starts

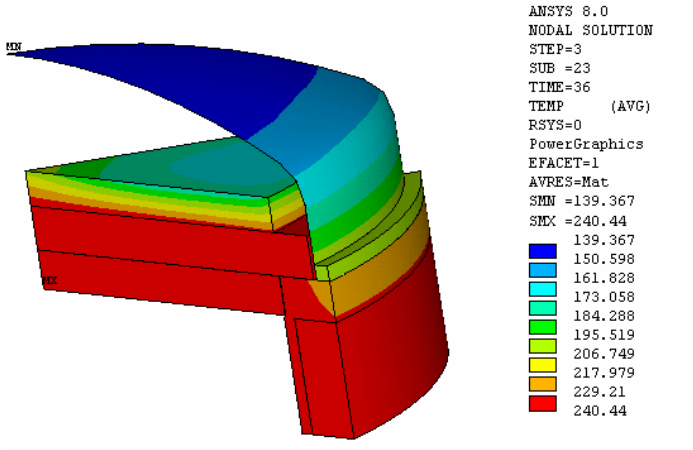

Figure 4.5-1
Time-Temperature History for the Vacuum Drying with 30 kW Decay Heat Load

a) Without Helium Backfilling

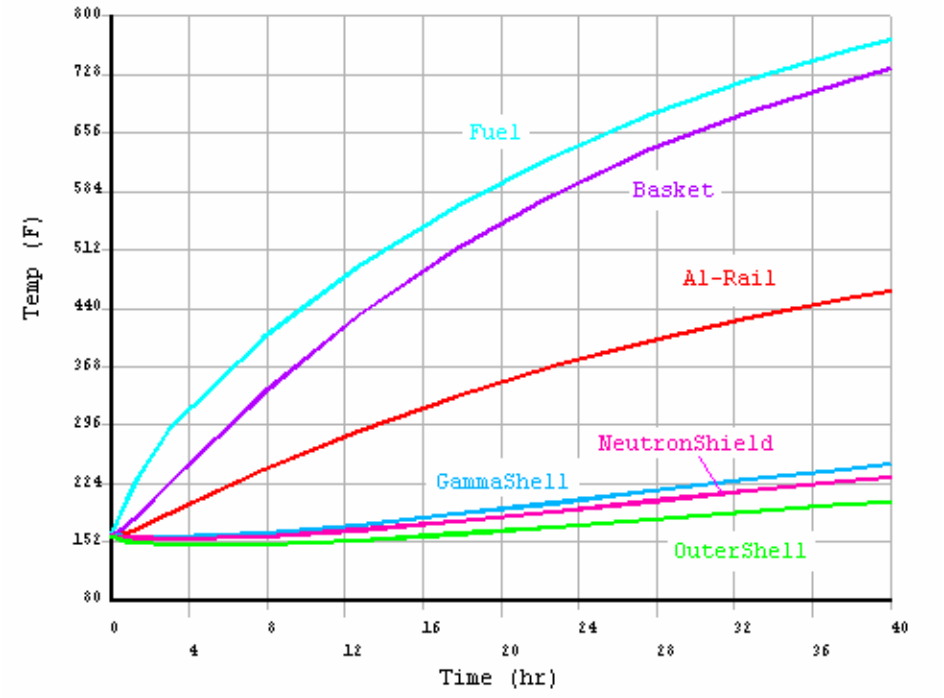

b) With Helium Backfilling at 30 Hours

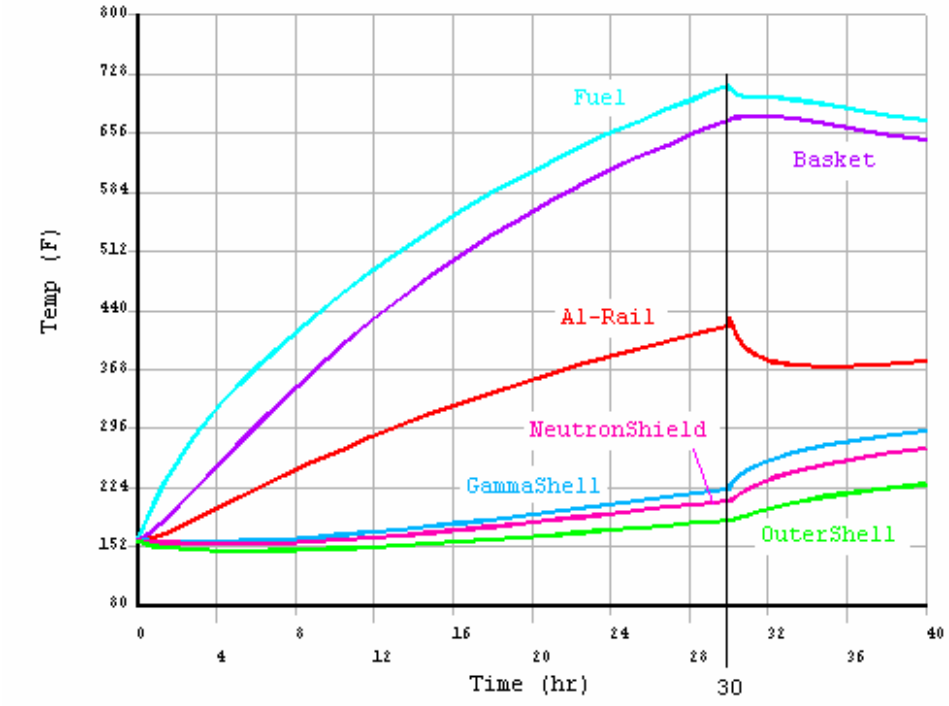

Figure 4.6-1
Location of the Damaged Fuel Assemblies

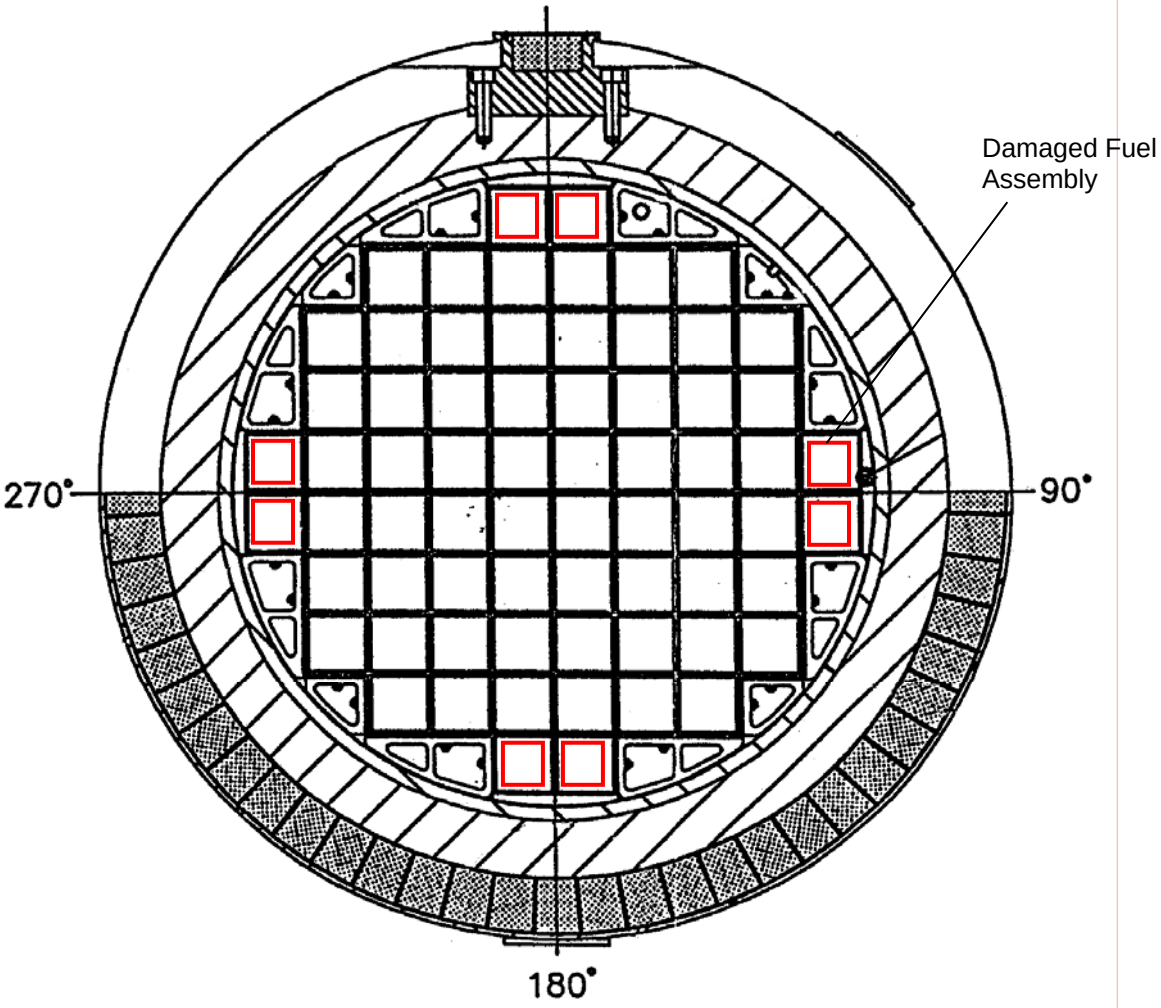

Figure 4.8-1
Comparison of the Transverse Effective Fuel Conductivities

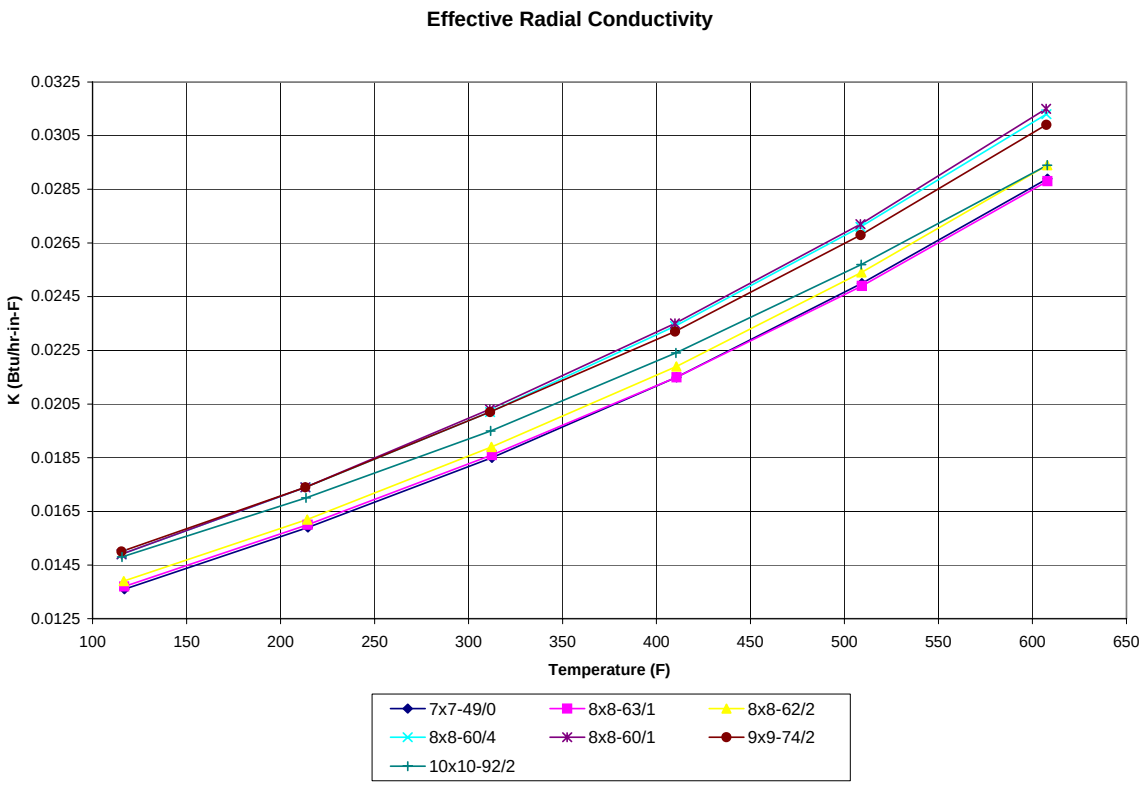

Figure 4.9-1
Comparison of the Measured and Applied Axial Heat Profiles

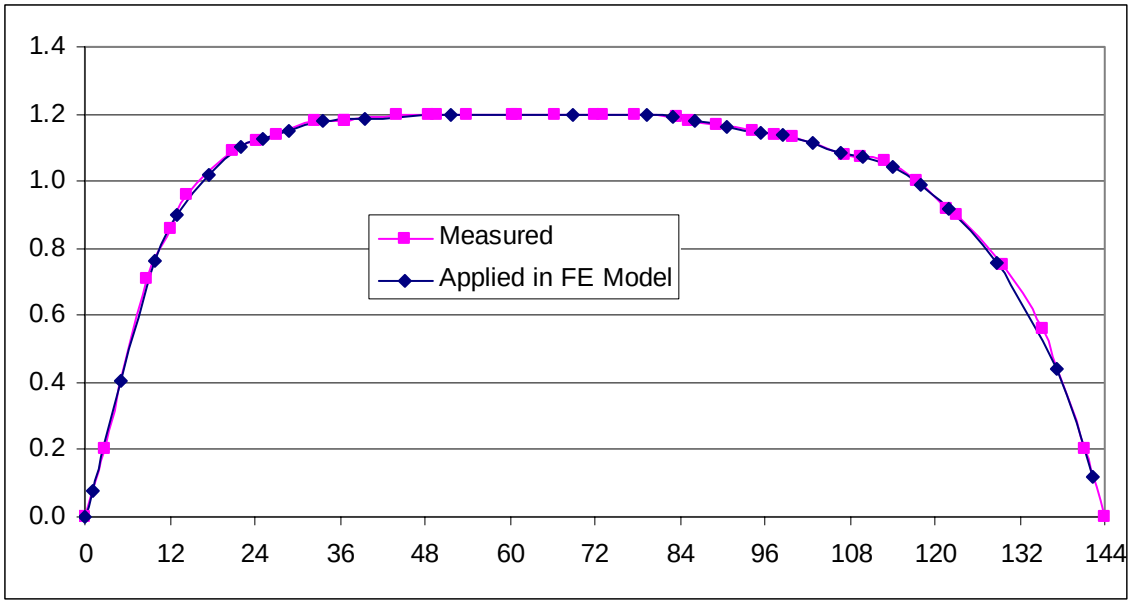

Figure 4.10-1
Storage Configuration for TN-68 Cask

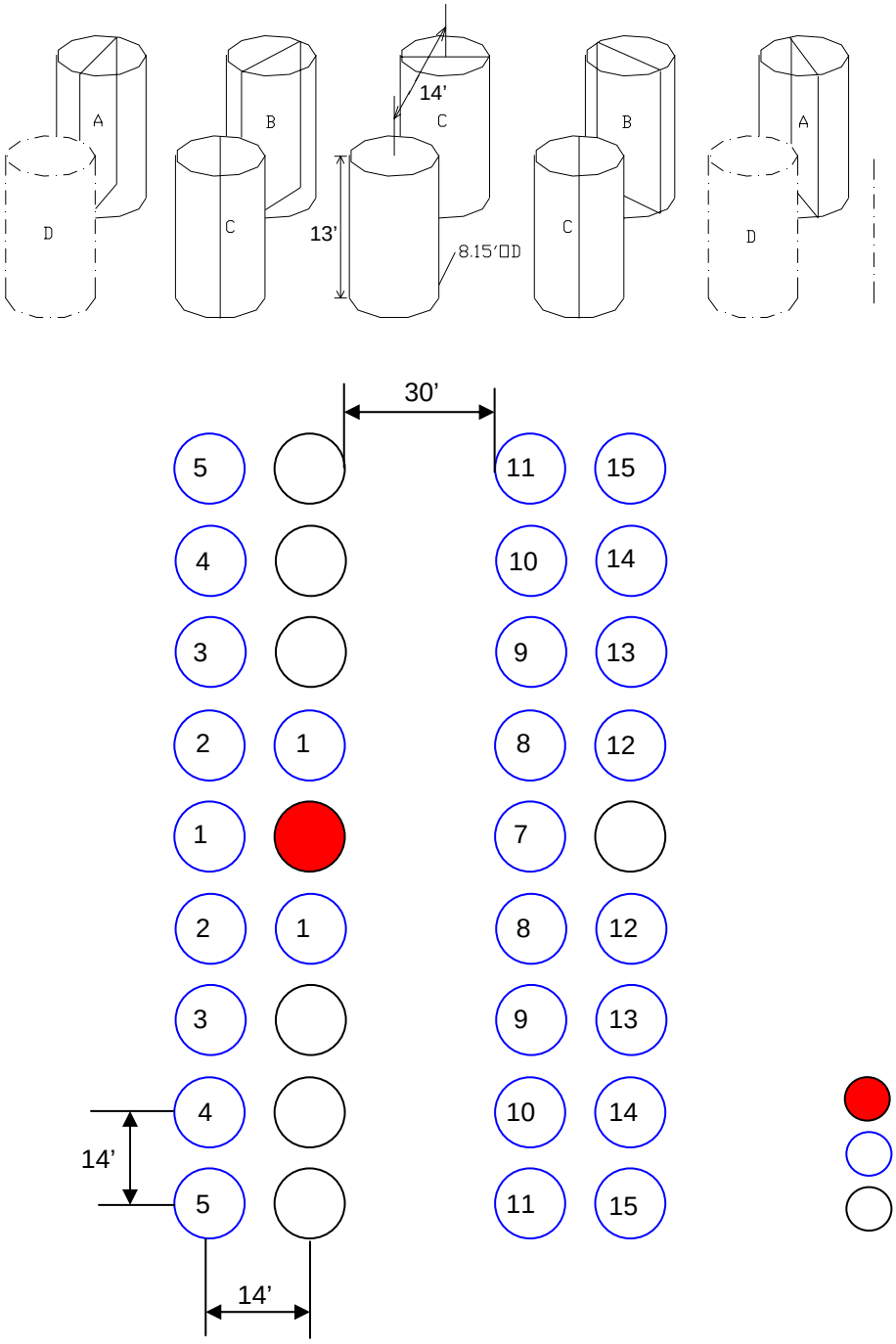

Figure 4.11-1
Considered Basket Locations for Calculation of Hot Gap Size